

Thermal axions with multi-eV masses are possible in low-reheating scenarios

Pierluca Carenza,^{a,b} Massimiliano Lattanzi,^c Alessandro Mirizzi,^{a,b}
Francesco Forastieri^{c,d}

^aDipartimento Interateneo di Fisica “Michelangelo Merlin”, Via Amendola 173, 70126 Bari, Italy

^bIstituto Nazionale di Fisica Nucleare - Sezione di Bari, Via Orabona 4, 70126 Bari, Italy

^cIstituto Nazionale di Fisica Nucleare, Sezione di Ferrara, Via Giuseppe Saragat 1, I-44122 Ferrara, Italy.

^dDipartimento di Fisica e Scienze della Terra, Università di Ferrara, Via Giuseppe Saragat 1, I-44122 Ferrara, Italy.

E-mail: pierluca.carenza@ba.infn.it, lattanzi@fe.infn.it,
alessandro.mirizzi@ba.infn.it, francesco.forastieri@unife.it

Abstract. We revise cosmological mass bounds on hadronic axions in low-reheating cosmological scenarios, with a reheating temperature $T_{\text{RH}} \leq 100$ MeV, in light of the latest cosmological observations. In this situation, the neutrino decoupling would be unaffected, while the thermal axion relic abundance is suppressed. Moreover, axions are colder in low-reheating temperature scenarios, so that bounds on their abundance are possibly loosened. As a consequence of these two facts, cosmological mass limits on axions are relaxed. Using state-of-the-art cosmological data and characterizing axion-pion interactions at the leading order in chiral perturbation theory, we find in the standard case an axion mass bound $m_a < 0.26$ eV. However, axions with masses $m_a \simeq 1$ eV, or heavier, would be allowed for reheating temperatures $T_{\text{RH}} \lesssim 80$ MeV. Multi-eV axions would be outside the mass sensitivity of current and planned solar axion helioscopes and would demand new experimental approaches to be detected.

Contents

1	Introduction	1
2	Thermal axions	2
2.1	Axion decoupling in standard cosmology	2
2.2	Axion decoupling in low-reheating scenario	4
3	Thermal axions and cosmological observables in low-reheating scenarios	7
4	Data and analysis	11
5	Results and discussions	13
6	Conclusions	17

1 Introduction

Cosmological observations, including measurements of the cosmic microwave background (CMB) anisotropies and of the distribution of large scale structures (LSS), are powerful tools to constrain the cosmic history of the universe. These precision measurements provide stringent bounds on particle physics models that seek to account for the matter and energy content of the observed Universe. In this context, a notable example is constituted by neutrino masses for which one gets cosmological bounds that are at least one order of magnitude more stringent than those obtained from laboratory searches [1–6]. The constraining potential of cosmological measurements has been subsequently applied to the case of other low-mass relics [7]. In this context, a case that has been studied for more than a decade is constituted by axion hot dark matter [8]. The analysis of axion mass bounds has been performed by different groups using an updated set of cosmological data [9–16] for hadronic axions models, most notably the Kim-Shifman-Vainshtein-Zakharov (KSVZ) axions [17, 18], where the QCD axion coupling to Standard Model fermions is negligible, since it vanishes at tree level. In particular, the latest analysis including the Planck 2018 data and the Baryon Acoustic Oscillations (BAO) measurements allows one to set a bound $m_a < 0.192$ eV at 95% C.L [19]. It has been also predicted that future cosmological surveys, like EUCLID would improve the sensitivity to axion mass bound, reaching $m_a \sim 0.15$ eV [15] which would be nicely complementary with the reach of the future laboratory experiments, like IAXO [20]. More recently the cosmological mass bounds have been considered also for models in which axions have a non negligible coupling with the electrons, like the Dine-Fischler-Srednicki-Zhitnisky (DFSZ) model [21, 22]. In this scenario, in [23] it has been shown that using the latest Planck and BAO data one would get a bound $m_a \lesssim 0.2$ eV when the axion-pion coupling is maximal. However, constraints on m_a may be significantly relaxed and possibly vanish if the axion-pion coupling is small. Furthermore, we note that future CMB experiments like CMB-S4 will open a new observational window on axions through their sensitivity to the effective number of relativistic degrees of freedom N_{eff} [24–26]. In the case of the QCD axion, this would allow to probe the region of masses $m_a \sim \mathcal{O}(\text{few})$ meV, or even smaller, depending on the particular realization of the model [24].

The tight cosmological mass bounds are competitive with, and often stronger than, those obtained from stellar energy loss arguments, and from direct laboratory experiments (see [27] for a recent review). However, a fundamental question is to assess how robust they are with respect to variations of the cosmological model. In this context, a common assumption about the history of the Universe is that its expansion was driven by relativistic particles at early epochs. This radiation-dominated era usually arises as a result of the thermalization of the decay products of a massive particle, a process called reheating. In the standard cosmological model, it is assumed that there was only one such an event, right after primordial inflation, and that it occurred at very large temperatures. However, we cannot *a priori* exclude that there was more than one of such an event, and that the last reheating episode occurred at much lower temperature than those usually associated to inflation. From a strictly observational point of view, the reheating temperature can be bounded from below using measurements of primordial element abundances and observations of the Cosmic Microwave Background (CMB). Previous analyses have shown the lower bound on the reheating temperature to be $\mathcal{O}(1 \text{ MeV})$ [28–33]. Therefore, it is still possible that unstable non-relativistic particles, other than the inflaton, were responsible of more than one reheating processes at different times in the evolution of the Universe, leading to a series of matter and radiation-dominated phases. In these *low-reheating* scenarios [34–36], our Universe could have reheated to a temperature as low as few MeV, postponing the beginning of the radiation-dominated epoch. The cosmological consequences of this model concerning dark matter production and baryogenesis have been widely explored (see, e.g. [37]). In particular, the consequences on non-thermal cold dark matter axion production and detection has been studied [38–41]. Low-reheating temperature would have also an impact on the decoupling of low-mass thermal relics. Notably, one can model these low-reheating scenarios through the decay of massive particles ϕ with a rate Γ_ϕ , leading to entropy generation. These decays would soften the time evolution of the temperature, increasing the Hubble parameter $H(T)$ and producing an earlier freeze-out of relic particles, suppressing their relic abundance due to entropy generation. This effect has been studied in the context of neutrinos (see, e.g., [28–31]), where latest analysis show a relaxation of the mass bound up to $\sum m_\nu < 1 \text{ eV}$ [31]. A more remarkable relaxation of the mass bound was predicted long time ago for axions by Grin, Smith & Kamionkowski [42] (hence thereafter, GSK08). Motivated by this seminal insight, we perform an updated study of axion mass bounds in low-reheating scenarios, using the latest cosmological measurements.

The plan of our work is as follows. In Section 2 we compare the axion thermalization in the standard case and in the low-reheating scenario. In Section 3 we discuss the cosmological observables in low-reheating scenarios for thermal axions. In Section 4 we present the cosmological data we use and we describe our analysis. In Section 5 we show and discuss our axion mass bounds in low-reheating scenarios. Finally, in Section 6 we discuss the phenomenological implications of our findings and we conclude. An Appendix follows in which we give more details on the axion decoupling in low-reheating scenario.

2 Thermal axions

2.1 Axion decoupling in standard cosmology

The most elegant solution to the *strong CP problem* is based on the Peccei-Quinn (PQ) mechanism [43–46], in which the Standard Model is enlarged with an additional global $U(1)_A$ symmetry, known as the PQ symmetry. The axion is the Nambu-Goldstone boson of the PQ

symmetry, a low-mass pseudoscalar particle with properties similar to those of neutral pions. Recent precision calculations based on chiral perturbation theory [47] or on lattice QCD [48] predict the axion mass as

$$m_a = \frac{5.7 \text{ eV}}{f_a/10^6 \text{ GeV}} , \quad (2.1)$$

where f_a is the axion decay constant or PQ scale. The axion interactions with photons, electrons, and hadrons are also controlled by the PQ constant and scale as f_a^{-1} . Therefore, the PQ scale determines the axion phenomenology and is constrained by different experiments and astrophysical arguments that involve interactions with photons, electrons, and hadrons (see [27, 49, 50] for recent reviews).

Apart from the original theoretical motivation, a renewed interest arose towards axions in the recent years since these still elusive particles can play a crucial role in explaining the dark matter (DM) puzzle in the Universe [51–54]. Indeed, depending on their mass and production mechanism, axions can play the role of both cold and hot dark matter relics. In particular, axions with masses in the range 10–1500 μeV might provide the dominant cold dark matter component, and would be searched by the ADMX [55, 56] and MADMAX [57] experiments. In this context their main production mechanism would be the non-thermal realignment, and depending on the cosmological scenario there can be some contribution associated with decays of topological defects, like cosmic strings and domain walls. Furthermore, for a Peccei-Quinn constant $f_a < 1.2 \times 10^{12} \text{ GeV}$, there would be also a primordial axion population produced in the hot thermal plasma [58–60]. In particular, if axions have masses $m_a \gtrsim 0.15 \text{ eV}$ (i.e. $f_a \lesssim 3.8 \times 10^7 \text{ GeV}$) they would decouple after the QCD phase transition ($T_{\text{QCD}} \simeq 200 \text{ MeV}$), as shown in Fig. 1 of [14]. In this case, their most generic interaction processes would involve pions rather than quarks and gluons present at earlier epochs [61, 62]. These processes would lead to a background of thermal axions, that would provide another hot dark matter component, in addition to active neutrinos.

In principle the region with $f_a < 4.0 \times 10^8 \text{ GeV}$ corresponding to $m_a > 15 \text{ meV}$ would be excluded from the observation of SN 1987A neutrinos [63, 64] (see also [65]). Indeed, an excessive axion emission via nucleon-nucleon bremsstrahlung in the supernova core, would have shortened the observed supernova neutrino burst. However, due to the sparseness of the supernova neutrino data and the uncertainties in the SN modeling at late time, this bound should be taken *cum grano salis*, and it is not redundant to investigate this region of the axion parameter space with other arguments. In this context, for models in which axions have a non negligible coupling with the electrons, like the DFSZ model [21, 22], there are different constraints from different stellar systems (e.g. red giants) which might even exclude masses larger than 10 meV in specific realizations of the model (see Fig. 12 of Ref. [66]). On the other hand, in the case of hadronic axion models, most notably the KSVZ axions [17, 18], the strong astrophysical constraints on the axion electron coupling [67, 68] provide only a weak bound on the PQ constant, since the coupling to electrons is suppressed by loop effects. Therefore, one has to rely on the weaker horizontal branch bound [69, 70], $g_{a\gamma} \lesssim 0.65 \times 10^{-10} \text{ GeV}^{-1}$, which translates into $f_a \geq 1.8 C_\gamma \times 10^7 \text{ GeV}$ (i.e., $m_a \leq 0.32 C_\gamma^{-1} \text{ eV}$), where C_γ is a model dependent constant. In this context, models have been proposed where C_γ is very small, relaxing the axion mass bound [71].

In the following we will focus on hadronic axions. Since these do not couple to charged leptons, their main thermalization process is given by the interactions with pions [8]

$$a + \pi \leftrightarrow \pi + \pi , \quad (2.2)$$

where the axion-pion interaction at the leading order based on effective field theory is described by the Lagrangian [62, 72–74] (see also [66])

$$\mathcal{L}_{a\pi} = \frac{C_{a\pi}}{f_\pi f_a} (\pi^0 \pi^+ \partial_\mu \pi^- + \pi^0 \pi^- \partial_\mu \pi^+ - 2\pi^+ \pi^- \partial_\mu \pi^0) \partial^\mu a , \quad (2.3)$$

where in hadronic axion models, the coupling constant $C_{a\pi} = (1 - z)/[3(1 + z)]$, with $z = m_u/m_d = 0.48$ is the ratio of up and down quark mass, and $f_\pi = 92$ GeV is the pion decay constant [47]. In a recent paper (Ref. [74]) the validity of the calculation of axion thermalization based on the leading order Lagrangian of Eq. (2.3) has been questioned for decoupling temperatures $T_D \gtrsim 62$ MeV. Indeed, in this case the effective field theory would break down. The authors of Ref. [74] propose using lattice QCD techniques to avoid a chiral expansion in regimes where its validity may fail. At this stage, however, there is no feasible alternative approach to estimate the thermal axion abundance. Therefore, we limit ourselves to the traditional treatment of axion thermalization presented in [8] and comment later on this important point.

Axion decoupling occurs when the interaction rate becomes slow compared with the cosmic expansion rate. We thus use as criterion for axion decoupling

$$\langle \Gamma_a \rangle = H(T) , \quad (2.4)$$

where $\langle \Gamma_a \rangle$ is the axion absorption rate, averaged over a thermal distribution at temperature T , whereas $H(T)$ is the Hubble expansion parameter at the cosmic temperature T :

$$H(T) = \left[\frac{4\pi^3}{45} g_*(T) \right]^{1/2} \frac{T^2}{m_{\text{Pl}}} . \quad (2.5)$$

Here, $g_*(T)$ is the effective number of thermal degrees of freedom that are excited at the epoch with temperature T , and $m_{\text{Pl}} = G_N^{-1/2}$ is the Planck mass. Our freeze-out criterion is accurate up to a constant of order unity. We notice that for decoupling temperatures $T_D > T_{\text{QCD}} \gtrsim 200$ MeV, the freeze-out epoch suddenly jumps to a much higher temperature because axion interactions with gluons and quarks before confinement are much less efficient [15]. When needed, we take into account the effect of the QCD phase transition in the effective degrees of freedom g_* following the treatment given in [75], while for simplicity we do not change the interaction rate. This choice does not affect our results since it involves a region of the parameter space where already the change in g_* is enough to suppress a thermal axion population frozen out before the QCD epoch.

Having determined the axion decoupling temperature T_D in this way, one can calculate the present-day axion number density by resorting to entropy conservation. This yields

$$n_a = \frac{g_{*S}(T_{\text{today}})}{g_{*S}(T_D)} \times \frac{n_\gamma}{2} , \quad (2.6)$$

where $g_{*S}(T)$ is the effective number of entropy degrees of freedom at temperature T , while $T_{\text{today}} = 2.73$ K and n_γ are the present-day temperature and number density of CMB photons.

2.2 Axion decoupling in low-reheating scenario

The axion thermalization described in the previous Section would be strongly affected in nonstandard cosmological histories, as pointed out in GSK08 [42]. A well-motivated class of

nonstandard cosmological histories, is constituted by those realized in low-reheating temperature scenarios. Details of axion thermalization in this case are given in the Appendix.

In low-reheating scenarios one considers a massive particles ϕ decaying with a rate Γ_ϕ into relativistic particles, reheating the Universe in the process. The equation for the energy density of ϕ is that of a decaying non-relativistic species [29]

$$\frac{d\rho_\phi}{dt} = -\Gamma_\phi \rho_\phi - 3H\rho_\phi . \quad (2.7)$$

One can define a reheating temperature T_{RH} as¹ [42]

$$\Gamma_\phi = H(T_{\text{RH}}) , \quad (2.8)$$

that marks the point where the Universe is already dominated by radiation with T_{RH} . From Eqs. (2.5) and (2.8) one obtains

$$T_{\text{RH}} \simeq 0.7 \left(\frac{g_*}{10.75} \right)^{-1/4} \left(\frac{\Gamma_\phi}{\text{s}^{-1}} \right) \text{ MeV} , \quad (2.9)$$

where we fixed g_* to its Standard Model value, neglecting the axion degree of freedom. This temperature gives a rough idea about the reheating temperature when the Universe enters the standard radiation dominated phase.

The outcome of our calculations do not depend on the choice of the initial time if $t_i \ll t(T_{\text{RH}})$, provided that the maximum value of temperature that is reached is significantly larger than the neutrino and axion decoupling temperature. The photon temperature T decreases as $t^{-1/4}$ when matter dominates and as $t^{-1/2}$ when relativistic particles fix the cosmological expansion. Therefore, the Universe expands faster during reheating than it would during radiation domination, the Hubble parameter being given by [42]

$$H = \sqrt{\frac{5\pi^3 g_*^2(T)}{9g_{*,\text{RH}}}} \left(\frac{T}{T_{\text{RH}}} \right)^2 \frac{T^2}{m_{\text{pl}}} , \quad (2.10)$$

where $g_{*,\text{RH}}$ are the thermal degree of freedom at the reheating temperature. Due to the faster Universe expansion, the equilibrium condition, $\langle \Gamma_a \rangle \gtrsim H(T)$ is harder to be maintained. Particles with decoupling temperatures $T_{\text{D}} \gtrsim T_{\text{RH}}$ come into chemical equilibrium, but then freeze out before reheating completes. Their abundances are then reduced by entropy production during reheating. In the specific case of axions, as the reheating temperature is lowered, axions freeze out at higher temperatures due to the higher value of H [42]. As the reheating temperature is increased, the $T \sim t^{-1/4}$ epoch becomes increasingly irrelevant and one would recover the standard axion-thermalization. As done in GSK08 [42], in the following we will limit ourselves to $T_{\text{RH}} \gtrsim 10$ MeV. For these values of the reheating temperature the neutrino decoupling proceeds as in the standard scenario [31].

In Fig. 1 we show the axion decoupling temperature T_{D} in function of the Peccei-Quinn scale f_a and the axion mass m_a for different reheating temperatures T_{RH} . The standard case corresponds to $T_{\text{RH}} = \infty$. We realize that for sufficiently high reheating temperature, $T_{\text{RH}} = 150$ MeV in the figure, the behaviour is identical to the standard case. Lowering the reheating temperature we find that for $T_{\text{D}} < T_{\text{RH}}$ the decoupling temperature coincides with the one obtained in the standard scenario. Conversely for $T_{\text{D}} > T_{\text{RH}}$ one finds a

¹Note that in other works, e.g. in [29], the reheating temperature has been defined through $\Gamma_\phi = 3H(T_{\text{RH}})$

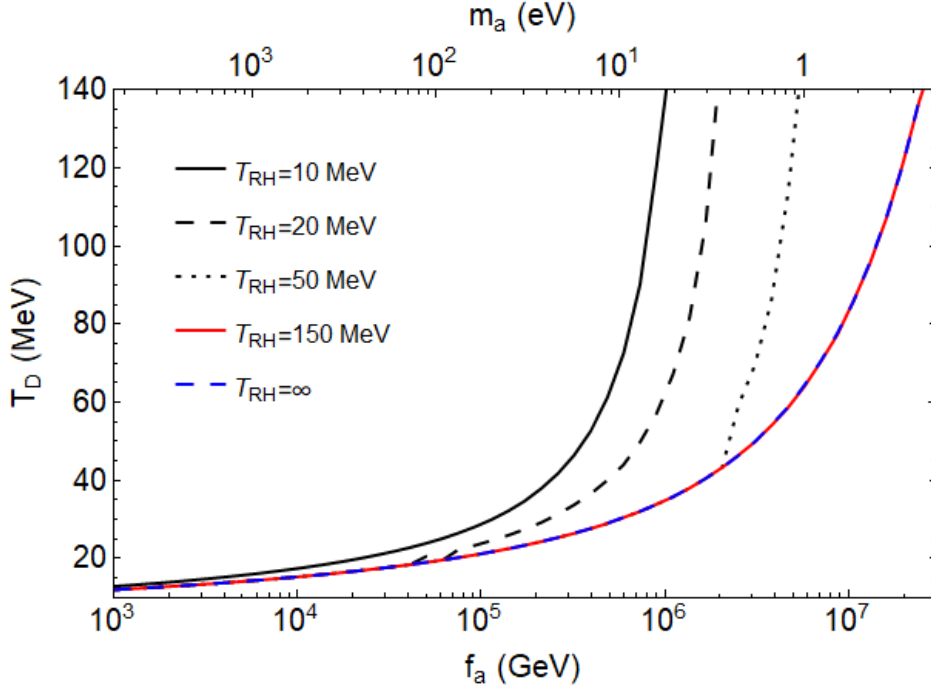


Figure 1. Axion decoupling temperature T_D in function of the Peccei-Quinn scale f_a and the axion mass m_a for different reheating temperatures T_{RH} .

higher decoupling temperature with respect to the standard case due to the higher Universe expansion rate.

From the decoupling temperature it is possible to calculate the present axion abundance as [42]

$$\Omega_a h^2 = \frac{m_a}{13 \text{ eV}} \frac{1}{g_{*,s}(T_D)} \times \begin{cases} \left(\frac{T_{RH}}{T_D}\right)^5 \left[\frac{g_*(T_{RH})}{g_*(T_D)}\right]^2 \left[\frac{g_{*,s}(T_D)}{g_{*,s}(T_{RH})}\right] & \text{for } T_D > T_{RH} \\ 1 & \text{for } T_D \leq T_{RH} \end{cases} \quad (2.11)$$

In Fig. 2 we plot the axion abundance $\Omega_a h^2$ in function of the Peccei-Quinn scale f_a and the axion mass m_a for different reheating temperatures T_{RH} . One realizes that lowering the reheating temperature the axion abundance gets significantly suppressed with respect to the standard case. In particular, the lower the reheating temperature T_{RH} the higher the axion mass for which one starts finding the suppression in the abundance. We also realize that for $T_{RH} < T_{QCD}$ MeV there is a change in the slope in $\Omega_a h^2$ that becomes milder at larger f_a . This change corresponds to axion decoupling occurring after the QCD phase transition.

Axions may also give contribution to extra-radiation, affecting the effective number of relativistic species N_{eff} . As long as $T_a \gg m_a$, this extra-contribution can be evaluated as [42]

$$\Delta N_{\text{eff}} = \left(\frac{4}{7}\right) \left(\frac{11}{4}\right)^{4/3} \times \begin{cases} \left(\frac{T_{RH}}{T_D}\right)^{20/3} \left[\frac{g_*(T_{RH})}{g_*(T_D)}\right]^{8/3} \left[\frac{g_{*,s}(T)}{g_{*,s}(T_{RH})}\right]^{4/3} & \text{for } T_D > T_{RH} \\ \left[\frac{g_{*,s}(T)}{g_{*,s}(T_D)}\right]^{4/3} & \text{for } T_D \leq T_{RH} \end{cases} \quad (2.12)$$

In Fig. 3 we show the axion extra-radiation ΔN_{eff} in function of the Peccei-Quinn scale f_a and the axion mass m_a for different reheating temperatures T_{RH} . In the standard case an

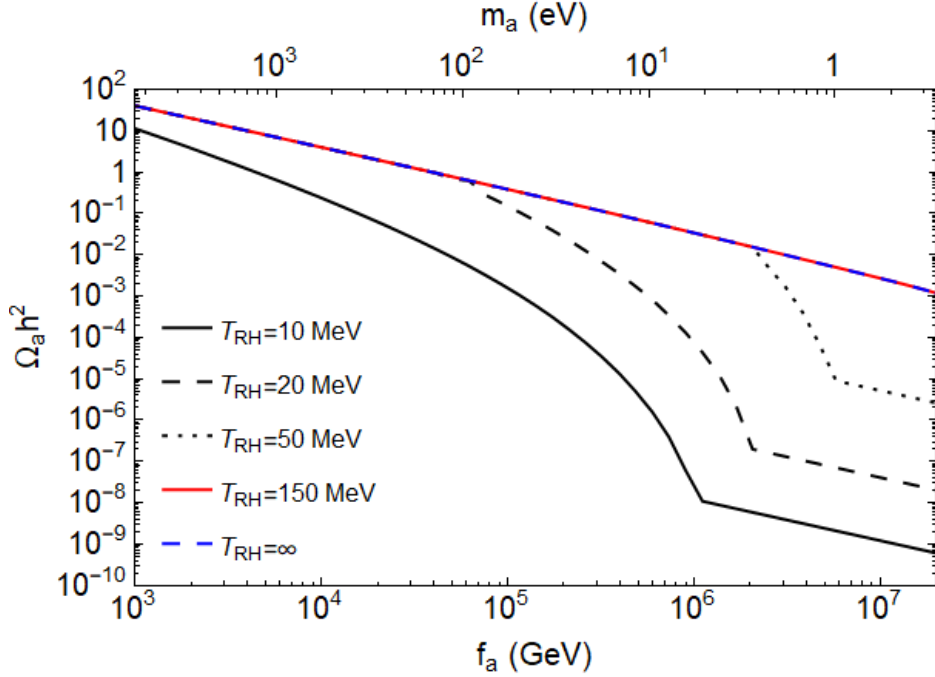


Figure 2. Present axion abundance $\Omega_a h^2$ in function of the Peccei-Quinn scale f_a and the axion mass m_a for different reheating temperatures T_{RH} .

axion with $m_a \sim 1$ eV would contribute with $\Delta N_{\text{eff}} \simeq 0.29$. Once more we realize that lowering the reheating temperature one finds a dramatic suppression of ΔN_{eff} with respect to the standard case.

3 Thermal axions and cosmological observables in low-reheating scenarios

We now build on the results presented in the previous sections, and describe the imprint of thermal axions in low-reheating scenarios on cosmological observables. In the standard scenario, thermal axions behave as hot dark matter, i.e., their average momentum $\langle p_a \rangle \sim T_a \gg m_a$ at the times of interest for structure formation. Their phenomenology is related to their large free-streaming length, and their imprint on cosmological observables is very similar to that of the active neutrinos. This is however not necessarily the case in low-reheating scenarios, as also noted in GSK08 [42]. In fact, when $T_{RH} \ll T_D$, the entropy generation occurring during the reheating stage can strongly suppress the axion-to-photon temperature ratio, effectively resulting in a much lower axion temperature with respect to the standard scenario, as we show in the following.

The axion-to-photon temperature ratio \mathcal{T}_a well after reheating and decoupling ($T \ll T_{RH}, T_D$) is given by

$$\mathcal{T}_a \equiv \frac{T_a}{T} = \begin{cases} \left(\frac{T_{RH}}{T_D} \right)^{5/3} \left[\frac{g_*(T_{RH})}{g_*(T_D)} \right]^{2/3} \left[\frac{g_{*S}(T)}{g_{*S}(T_{RH})} \right]^{1/3} & \text{for } T_D \gg T_{RH}, \\ \left[\frac{g_{*S}(T)}{g_{*S}(T_D)} \right]^{1/3} & \text{for } T_D \ll T_{RH}. \end{cases} \quad (3.1)$$

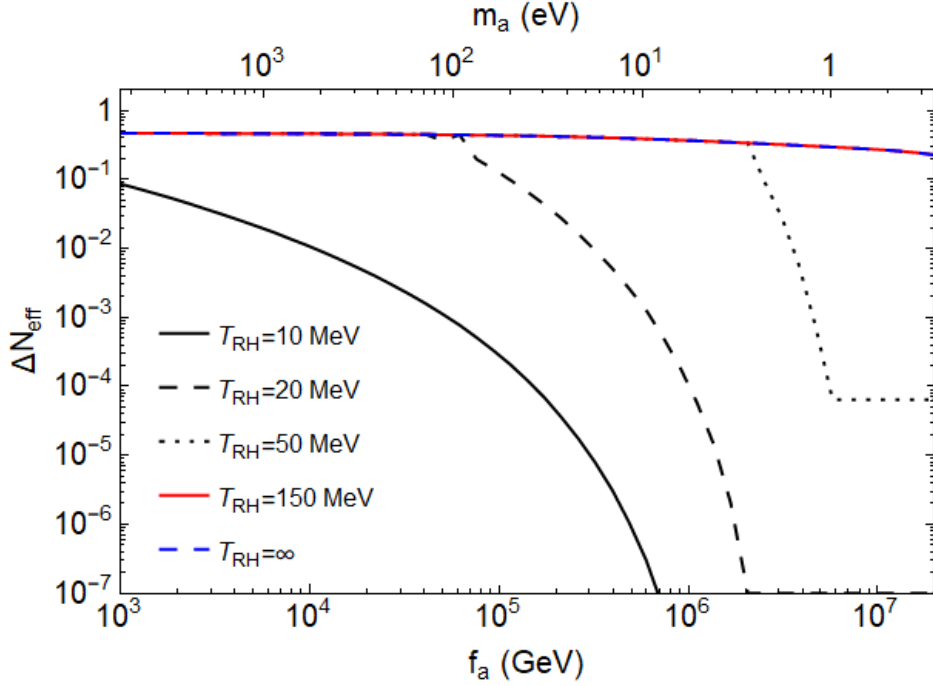


Figure 3. Axion extra-radiation ΔN_{eff} at $T = 1$ keV in function of the Peccei-Quinn scale f_a and the axion mass m_a for different reheating temperatures T_{RH} .

From this, the thermally-averaged ratio of axion momentum to mass at a given redshift z can be readily computed as

$$\frac{\langle p_a \rangle}{m_a} = 2.7 \frac{T_{\text{today}}(1+z)}{m_a} \times \begin{cases} \left(\frac{T_{\text{RH}}}{T_D} \right)^{5/3} \left[\frac{g_*(T_{\text{RH}})}{g_*(T_D)} \right]^{2/3} \left[\frac{g_*(T_{\text{today}})}{g_*(T_{\text{RH}})} \right]^{1/3} & \text{for } T_D \gg T_{\text{RH}}, \\ \left[\frac{g_*(T_{\text{today}})}{g_*(T_D)} \right]^{1/3} & \text{for } T_D \ll T_{\text{RH}}, \end{cases} \quad (3.2)$$

where we have used $\langle p_a \rangle = 2.7 T_a$ for bosons, $T \propto g_{*s}^{1/3}(1+z)$. It is clear from the above expression that the ratio $\langle p_a \rangle/m_a$ can be much smaller with respect to the standard case when $T_D \gg T_{\text{RH}}$. This behavior is shown in Fig. 4 for an axion mass $m_a = 1$ eV, at the redshift of matter-radiation equality $z_{\text{eq}} \simeq 3400$.

The cosmological phenomenology of axions, and of relic particles in general, crucially depends on the value of $\langle p_a \rangle/m_a$ at the times probed by observations. In the standard case $\langle p_a \rangle/m_a \gg 1$ for a large fraction of the cosmic history for thermal axions, and these behave as *hot dark matter*. In this scenario the axion density is severely constrained both by CMB measurements of N_{eff} , and by their potential effect on structure formation, requiring that only a subdominant component of the total matter density can be contributed by particles with a large velocity dispersion. In low-reheating scenarios, however, the condition $\langle p_a \rangle/m_a \ll 1$ might be realized even at early times, and thermal axions would effectively behave as *cold dark matter*. In this scenario, axions would not contribute to N_{eff} , and bounds on their density would come only from the (weaker) requirement that this should not exceed the cold dark matter density inferred e.g. through measurements of CMB anisotropies.

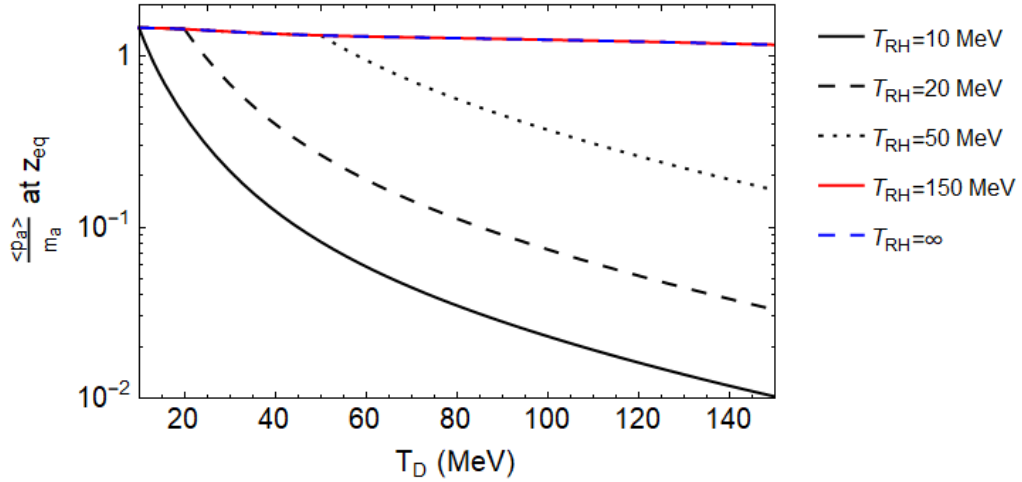


Figure 4. Axion average momentum-to-mass ratio $\langle p_a \rangle / m_a$ at redshift $z_{\text{eq}} = 3400$ and for an axion mass $m_a = 1$ eV in function of the decoupling temperature for different reheating temperatures T_{RH} .

A good proxy to assess the “hot” or “cold” nature of a relic is its behaviour at the time of matter-radiation equality² $z_{\text{eq}} \simeq 3400$, when the growth of density perturbations effectively starts.³ For example, in their classic textbook Kolb & Turner [77] compare the free-streaming length of the relic at z_{eq} to the Hubble radius at the same time, as a criterion to discriminate hot and cold dark matter. Similarly, one could evaluate the average momentum-to-mass ratio at z_{eq} .

We show in Fig. 5 the $\langle p_a \rangle / m_a$ ratio evaluated at $z = 3400$ as a function of the axion mass m_a (left panel) and energy density $\Omega_a h^2$ (right panel), for different values of the reheating temperature. Let us first examine the two extreme cases, i.e. the standard thermal history with $T_{\text{RH}} = \infty$ and the very low reheating scenario with $T_{\text{RH}} = 10$ MeV. In the former case, the average momentum-to-mass ratio decreases with axion mass, with axions lighter than ~ 1.4 eV having $\langle p_a \rangle / m_a > 1$ at z_{eq} . In terms of axion density, a mass of 1.4 eV corresponds to $\Omega_a h^2 \simeq 7 \times 10^{-3}$ for $T_{\text{RH}} = \infty$. Let us compare this value to observational limits on the density of hot relics. As a rough guide, we consider the upper bound on the sum of neutrino masses $\sum m_\nu < 0.257$ eV (at 95% CL) from Planck 2018 temperature and polarization data [76], and recast it as a bound on the present density parameter Ω_h of hot relics other than active neutrinos. After subtracting the contribution of active neutrinos with the minimum mass allowed by flavour oscillation experiments $\sum m_\nu = 0.06$ eV [4], we obtain $\Omega_a h^2 \leq \Omega_h h^2 \lesssim 2 \times 10^{-3}$, corresponding to $m_a \lesssim 0.45$ eV and $\langle p_a \rangle / m_a (z = z_{\text{eq}}) \simeq 3$. This limit should apply to hot axions, which is certainly the case for $m_a < 1.4$ eV. Hot axions should also satisfy observational constraints on N_{eff} . Imposing $\Delta N_{\text{eff}} < 0.35$, roughly corresponding to the 95% credible upper limit from the Planck 2018 data [76], yields $m_a < 0.96$ eV. This is of the same magnitude, albeit larger, than the limit coming from the present density of hot dark matter, so we can expect that combining the two requirements will yield

²Note that, in principle, the redshift of matter-radiation equality depends on the cosmological parameters and in particular on m_a . However, for the purpose of the qualitative considerations made in this section, we fix this quantity to its Λ CDM estimate from Planck 2018 [76].

³During the radiation era, density perturbations inside the horizon can grow logarithmically, at most (Meszaros effect).

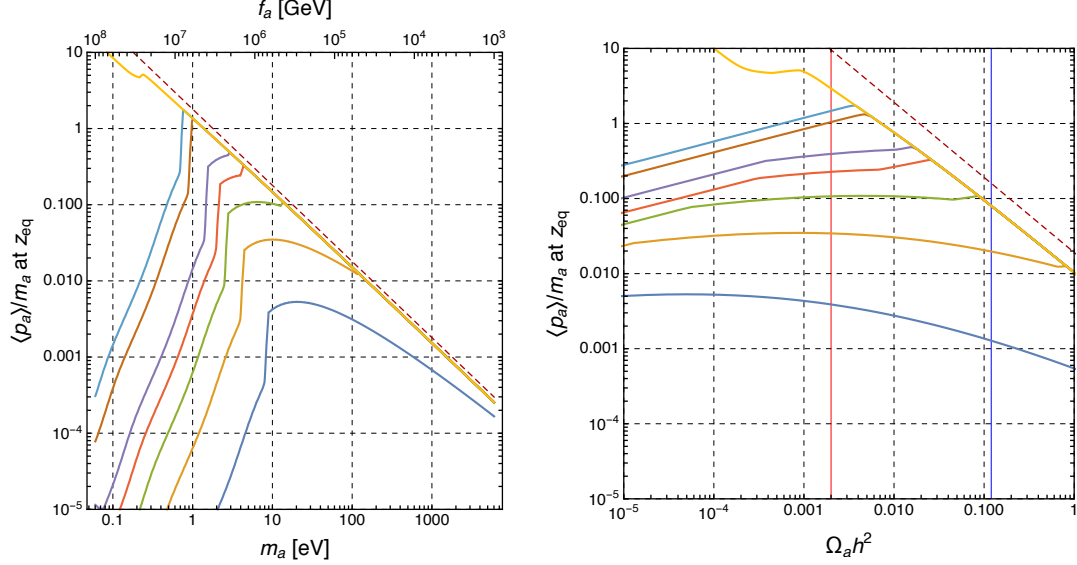


Figure 5. Left panel: Axion momentum-to-mass ratio at redshift $z_{\text{eq}} = 3400$, as a function of the Peccei-Quinn scale f_a and the axion mass m_a for different reheating temperatures T_{RH} . From top to bottom: $T_{\text{RH}} = (\infty, 100, 80, 50, 40, 30, 20, 10)$ MeV. For comparison, the same quantity for active neutrinos is also shown (uppermost dashed curve). Right panel: same as left panel, but as a function of $\Omega_a h^2$. The vertical red and blue lines correspond to the reference values $\Omega_a h^2 = 2 \times 10^{-3}$ and $\Omega_a h^2 = 0.12$, roughly marking the upper limits on the density of a hot ($\langle p_a \rangle / m_a \gg 1$), or cold ($\langle p_a \rangle / m_a \ll 1$) axion, respectively (see text for discussion).

an upper limit on m_a somehow smaller than 0.45 eV. Let us now consider the mass range $m_a > 1.4$ eV, where $\langle p_a \rangle / m_a < 1$. Increasing the mass, a regime will be eventually reached where $\langle p_a \rangle / m_a \ll 1$. Here, thermal axions are cold and the relevant bound comes from requirement that their density should not overshoot the value of the cold dark matter density measured by Planck, $\Omega_a h^2 \leq \Omega_c h^2 = 0.1202 \pm 0.0014$. Since this is a looser requirement than $\Omega_a h^2 \lesssim 2 \times 10^{-3}$, in principle it might happen that another allowed region of axion masses exists for $m_a > 1.4$ eV. A closer inspection shows that this is probably not the case for $T_{\text{RH}} = \infty$. In fact, the value $\Omega_a h^2 = 0.12$ is reached for $m_a \simeq 20$ eV and $\langle p_a \rangle / m_a \simeq 0.1$. Such a value of $\langle p_a \rangle / m_a$ indicates that axions are still “warm” at equality (i.e. that their free-streaming length is a sizeable fraction of the Hubble radius). To reach the region in which thermal axions behave as cold, we should go to values of $\Omega_a h^2 > 0.12$, at variance with Planck observations. Let us now turn our attention to the scenario with a reheating temperature $T_{\text{RH}} = 10$ MeV. In this case, the average momentum-to-mass ratio at $z = 3400$ is at most $\lesssim 5 \times 10^{-3}$. We can expect that in this case the thermal axion phenomenology is essentially that of a cold particle, and thus the only relevant constraint is $\Omega_a h^2 \lesssim 0.12$, or $m_a \lesssim 410$ eV.

Based on these considerations, we can draw the following general picture, that should apply also to the scenarios in between the two that have been analysed above. At fixed reheating temperature, the axion mass uniquely fixes the values of $\Omega_a h^2$, ΔN_{eff} and $\langle p_a \rangle / m_a$. We expect the likelihood to be a decreasing (or at least, non-increasing) function of all these quantities. Note also that while $\Omega_a h^2$ and ΔN_{eff} grow monotonically with m_a , $\langle p_a \rangle / m_a$ does not necessarily share this feature, as it can be seen from Fig. 5. Thus, in principle it might be possible that, in addition to the expected minimum in $m_a \simeq 0$, the likelihood also has a

local minimum at $m_a \neq 0$ and that two disconnected allowed regions for m_a exist. We will see that at the end this is not realized in practice, nevertheless this has been an important point to keep in mind when performing Monte Carlo runs for parameter estimates.

Let us conclude by stressing that the above considerations are qualitative, as it should be clear that the transition from the hot to cold behaviour is a continuous one. Thus we might find that in some part of the parameter space the relevant limits on the axion density parameter $\Omega_a h^2$ and contribution to N_{eff} lie somewhere in between those for a hot and cold species. It is also not immediate to estimate the values of $\langle p_a \rangle / m_a (z = z_{\text{eq}})$ that are, observations-wise, indistinguishable from the limiting cases $\langle p_a \rangle / m_a = 0$ (cold) and $\langle p_a \rangle / m_a = \infty$ (hot). However, this is not a problem given the qualitative nature of the considerations made in this section, whose purpose is only to understand what to expect from the limits that will be derived in the next section through a Boltzmann code that precisely tracks the evolution of cosmological perturbation.

4 Data and analysis

We use the most up-to-date available observations of CMB temperature and polarization anisotropies, possibly in combination with baryon acoustic oscillation (BAO) measurements from galaxy surveys, in order to derive bounds on axion masses in low-reheating scenarios. In particular, we consider CMB observations from the Planck 2018 legacy data release⁴ [78] together with BAO measurements from BOSS Data Release 12 [79], 6dFGS [80] and SDSS-MGS [81]. Our baseline dataset consists of the combination of the Planck **Plik** likelihood using TT, EE and TE power spectra at multipoles $\ell \geq 30$, and of the **Commander** and **SimAll** likelihoods for temperature and EE polarization, respectively, at low- ℓ 's ($\ell < 30$) [82]. This combination is labeled Planck TT,TE,EE+lowE in the Planck collaboration papers; however, for the sake of brevity we will denote it simply as “PlanckTTTEEE”. However, here and in the following, use of the low- ℓ polarization data should be always understood. In fact, large-scale polarization data are needed in order to constrain the optical depth to reionization, τ ; this is particularly important for our analysis, since τ is degenerate with the abundance of hot relics.

In addition to the baseline, we consider two other datasets. In the first, the baseline is augmented by the Planck lensing likelihood [83]: we call this combination “PlanckTTTEEE+lensing”. In the second, labeled “PlanckTTTEEE+BAO” we add to PlanckTTTEEE the BAO data described above.

We use a modified version of the Boltzmann code **camb** to compute theoretical predictions for a given cosmological model. It is well known that the public version of **camb** allows for the inclusion of the effects of massive neutrinos in the evolution of cosmological perturbations. Through a suitable remapping of the neutrino parameters, this feature can in fact be extended to include hot or warm relics with a distribution proportional to a Fermi-Dirac, in practice treating them as “effective neutrinos” [84]. This property has been used, for example, in analyses aiming to derive cosmological bounds on sterile neutrinos, including the one reported in the Planck collaboration papers. However, an exact treatment of bosonic relics is not a feature of the public **camb** version, because the distribution function of hot/warm relics cannot be changed by the user. One can still resort to the “effective neutrino” approach, that however is only approximate, instead than being exact as in the case of fermions. For this work, instead, we have modified **camb** so that the code correctly uses a Bose-Einstein

⁴Data available at this url: <http://pla.esac.esa.int/pla>.

distribution for axions. In this way, once the axion parameters (essentially the present axion density and their contribution to N_{eff}) are specified, all other quantities (firstly mass and temperature, and secondly the various integrals over the distribution function) are computed consistently.

We consider a family of one-parameter extensions to the standard Λ CDM cosmological model, labeled Λ CDM+ m_a in which we allow for the presence of thermal axions. In each of these extensions the reheating temperature is fixed; in particular, we consider the values $T_{\text{RH}} = \{10, 20, 30, 40, 50, 80, 100\}$ MeV, and the case of a standard thermal history, as above referred as $T_{\text{RH}} = \infty$. These models could in principle be described by extending the usual Λ CDM parameterization with the axion mass, thus in terms of seven cosmological parameters: the baryon density $\omega_b \equiv \Omega_b h^2$, the cold dark matter (CDM) density $\omega_c \equiv \Omega_c h^2$, the angle subtended by the sound horizon at recombination θ_s , the optical depth to reionization τ , the logarithmic amplitude $\log(10^{10} A_s)$ and the spectral index n_s of the spectrum of primordial scalar perturbations. However, we find that a better parametrization can be obtained by trading the CDM density for the total CDM+axions density $\omega_{c+a} \equiv \omega_c + \omega_a$. The reason is that, for some values of the reheating temperature considered here, axions behave as cold particles, as explained in the previous section⁵. In this case ω_c and ω_a are strongly degenerate, because only their sum, the total abundance of cold particles, is actually constrained by the data. Thus we prefer to use ω_{c+a} as a base parameter, and derive the CDM abundance from $\omega_c = \omega_{c+a} - \omega_a$ (the latter being itself a derived parameter computed from m_a). In conclusion, this is the vector of base parameters, that take implicit flat priors in our Monte Carlo runs: $\{\omega_b, \omega_{c+a}, \theta_s, \tau, \log(10^{10} A_s), n_s, m_a\}$. We consider one massive and two massless active neutrino species, with a fixed sum of neutrino masses $\Sigma m_\nu = 0.06$ eV. The three active neutrino species contribute the standard value $N_{\text{eff}} = 3.046$ to the energy density of relativistic species after Big Bang Nucleosynthesis (BBN)⁶. We assume flatness and adiabatic initial conditions.

We use the Markov Chain Monte Carlo engine **CosmoMC**, interfaced with our modified version of **camb** and with the likelihood modules described above, to explore posteriors and derive estimates and uncertainties for the parameters of the model, and in particular to obtain bounds on the axion mass in low-reheating scenario. In addition to the base parameters, we also include nuisance parameters required by the likelihoods, that are eventually marginalized over. We check convergence of the chains by monitoring the Gelman-Rubin $R-1$ parameter. We also check stability of the limits on m_a obtained by considering each chain of a given run, one at a time.⁷ Moreover, since we might expect that the distribution is multimodal, for each model/dataset combination we perform (at least) two twin runs, one with Monte Carlo temperature⁸ $T_{\text{MC}} = 1$ and the other with $T_{\text{MC}} > 1$ (we usually take $T_{\text{MC}} = 2$ or 3). Setting the Monte Carlo temperature to a value other than 1 amounts to sample from $\mathcal{P}^{1/T}$ instead than from \mathcal{P} , with the latter being the posterior probability distribution of the parameters. Once the chains have been generated, they are importance weighted (“cooled”) to provide samples from the posterior \mathcal{P} . This procedure makes it easier to sample multimodal distributions, at the expense of a slower convergence. We use the “high- T_{MC} ” runs to check for the existence of separate peaks in the probability distribution (possibly corresponding to

⁵Note that we always use “CDM” to indicate the “non-axionic” component of DM.

⁶Refined calculations [85, 86] have recently modified this value to $N_{\text{eff}} = 3.044$, but the difference is not relevant for the datasets considered in this work.

⁷We usually generate 6 chains for each parameter estimation run.

⁸Not to be confused with the reheating temperature.

	PlanckTTTEEE	PlanckTTTEEE+lensing	PlanckTTTEEE+BAO
$T_{\text{RH}} = 10 \text{ MeV}$	< 391	< 393	< 391
$T_{\text{RH}} = 20 \text{ MeV}$	< 39.2	< 36.6	< 36.0
$T_{\text{RH}} = 30 \text{ MeV}$	< 6.72	< 6.55	< 6.31
$T_{\text{RH}} = 40 \text{ MeV}$	< 3.23	< 3.22	< 3.05
$T_{\text{RH}} = 50 \text{ MeV}$	< 2.09	< 2.05	< 1.89
$T_{\text{RH}} = 80 \text{ MeV}$	< 0.912	< 0.906	< 0.901
$T_{\text{RH}} = 100 \text{ MeV}$	< 0.691	< 0.696	< 0.688
$T_{\text{RH}} = \infty$	< 0.837	< 0.639	< 0.259

Table 1. 95% CL upper bounds on axion mass m_a (in eV) from different datasets, for the values of the reheating temperature T_{RH} indicated in the first column.

hot and cold axions). We also check consistency of the limits obtained between each pair of twin runs.

5 Results and discussions

Upper limits on the axion mass in low reheating scenarios are reported in Table 1 for different values of the reheating temperature, for the dataset combinations described in the previous section. The corresponding 1-dimensional posterior probability distributions are shown in Fig. 6.

We start by discussing the constraints obtained from the PlanckTTTEEE dataset. In the most extreme scenario that we consider, $T_{\text{RH}} = 10 \text{ MeV}$, the upper bound⁹ on the axion mass is relaxed to $m_a < 391 \text{ eV}$. As anticipated in the previous sections, this is due to fact that the axion energy density and velocity dispersion are both suppressed with respect to the standard scenario (see Figs. 2 and 5). Thus, axions are less abundant for a given mass and lower reheating temperatures; on top of that, they are also colder, so that observational limits on the abundance are relaxed. In fact, $m_a = 391 \text{ eV}$ and $T_{\text{RH}} = 10 \text{ MeV}$ yield $\omega_a = 0.108$, i.e. axions making up for nearly all the DM content of the Universe. This is in agreement with the low average momentum-to-mass ratio (always smaller than 10^{-2} at the time of equality) shown in Fig. 5. For a larger value of the reheating temperature $T_{\text{RH}} = 20 \text{ MeV}$, we find the upper bound $m_a < 39 \text{ eV}$, corresponding to $\omega_a = 0.057$. In this case axions can make up for a large fraction of the DM, but not all of it. We relate this finding to the larger velocity dispersion (i.e., axions are warmer) with respect to the $T_{\text{RH}} = 10 \text{ MeV}$ scenario. This trend continues as the reheating temperature increases, and axions of a given mass became warmer and more abundant. The upper bound in the $T_{\text{RH}} = 50 \text{ MeV}$ scenario is $m_a < 2.1 \text{ eV}$, corresponding to $\omega_a = 2.4 \times 10^{-3}$. The latter value is of the same order of magnitude as the maximum energy density in active neutrinos allowed by Planck data. This is again supported by a visual inspection of Fig. 5, from which the relatively large ratio at equality $\langle p_a \rangle / m_a \simeq 0.4$, can be read for $m_a \simeq 2 \text{ eV}$ and $T_{\text{RH}} > 50 \text{ MeV}$; this is just a factor of 2 smaller than the corresponding value for active neutrinos in the standard scenario (blue curve in the same figure). Further increasing the reheating temperature yields $m_a < 0.91 \text{ eV}$ ($T_{\text{RH}} = 80 \text{ MeV}$) and $m_a < 0.69 \text{ eV}$ ($T_{\text{RH}} = 100 \text{ MeV}$). For these values of the reheating temperature, the axion density is varying very quickly with m_a when the latter is close to

⁹Unless otherwise stated, the upper bounds discussed in the following always correspond to 95% Bayesian credible intervals.

the quoted upper limits, so it is not instructive to express these numbers in terms of ω_a . Finally, we obtain $m_a < 0.84 \text{ eV}$ for the standard thermal history. This bound is actually looser than the one found for $T_{\text{RH}} = 100 \text{ MeV}$. This seemingly counterintuitive result can be understood as follows. Let us consider how ω_a varies with m_a in the two cases; this is shown in the left panel Fig. 7. As above, we take 2×10^{-3} as a benchmark for the upper limit of hot relics allowed by Planck data. We do not need this value to be too precise for the argument that we are going to make. This threshold is reached for $m_a = 0.75 \text{ eV}$ ($T_{\text{RH}} = 100 \text{ MeV}$) or $m_a = 0.45 \text{ eV}$ ($T_{\text{RH}} = \infty$). Thus the observational limit is indeed violated sooner in the standard case with respect to $T_{\text{RH}} = 100 \text{ MeV}$. The upper limits on m_a are however also determined by the shape of the posterior curves, which is quite different in the two cases, as it can be seen in the last two panels of Fig. 6. It can be seen in Fig. 7 that, for $T_{\text{RH}} = 100 \text{ MeV}$, the axion density is strongly suppressed and basically negligible for $m_a < 0.7 \text{ eV}$. It then grows very quickly as the mass grows beyond this value, immediately overshooting the observational bound. The likelihood as a function of m_a will thus be constant and equal to its value in $m_a = 0$ up to $m_a = 0.7 \text{ eV}$, and then suddenly goes to zero for $m_a \gtrsim 0.7 \text{ eV}$. This reflects in the shape of the posterior. In the standard case, the axion density is increasing more smoothly as a function of m_a . Thus the likelihood peaks at $m_a = 0$ but starts decreasing as soon as we move away from this value. There is however a relatively long tail related to the fact that axions become colder as the mass increases, and this somehow compensates for the larger density. This explains the different shape of the posteriors between $T_{\text{RH}} = 100 \text{ MeV}$ and $T_{\text{RH}} = \infty$. It should be clear at this point that the region in m_a encompassing the 95% of the total posterior volume (the 95% Bayesian credible interval) can indeed be larger for $T_{\text{RH}} = \infty$ than for $T_{\text{RH}} = 100 \text{ MeV}$. For the sake of clarity, we show the two posteriors together in the right panel of Fig. 6, normalized so that they both integrate to unity.

Let us now comment on the bounds that we obtain from the extended datasets including also information from CMB lensing or BAO. Both additional datasets are particularly useful to constrain the abundance of light relics, either through their effect on structure formation (lensing) or by limiting possible changes to the expansion history (BAO). One might thus expect to find tighter constraints on the axion mass in at least some of the scenarios considered here, namely those in which the phenomenology of thermal axions is essentially that of a hot or warm particle. By looking at the values reported in Table 1 for low-reheating scenarios, we see that no significant improvement is observed for the PlanckTTTEEE+lensing dataset, with the exception of the $T_{\text{RH}} = 20 \text{ MeV}$ case; even in that case, it is quite marginal ($\sim 7\%$). For the PlanckTTTEEE+BAO dataset, the bounds improve in low-reheating scenarios with $20 \text{ MeV} \leq T_{\text{RH}} \leq 50 \text{ MeV}$, but also in this case the improvement is at most $\sim 10\%$ with respect to the value for PlanckTTTEEE+lensing. The fact that there is no improvement for $T_{\text{RH}} = 10 \text{ MeV}$ can be easily understood from the fact, noted above, that in this case axions behave as cold particles and can make all the DM. Thus the relevant observational bound is the upper limit on the DM density that is not significantly improved by the inclusion of lensing or BAO data.¹⁰ For what concerns larger reheating temperatures, it is true that in these cases the axion phenomenology is that of a warm/hot particle; however, the axion density is a very steep function of mass around in the region around the observational upper limits, so the effects of tighter constraints on ω_a (the quantity more directly probed by observations) are strongly diluted when translated in terms of m_a . The steepness of the (ω_a, m_a) relation

¹⁰Note that this statement holds for ω_a since this is bound to be $\leq \omega_{\text{cdm}}$. The Planck determination of ω_{cdm} itself is indeed made more precise by the inclusion of BAO data.

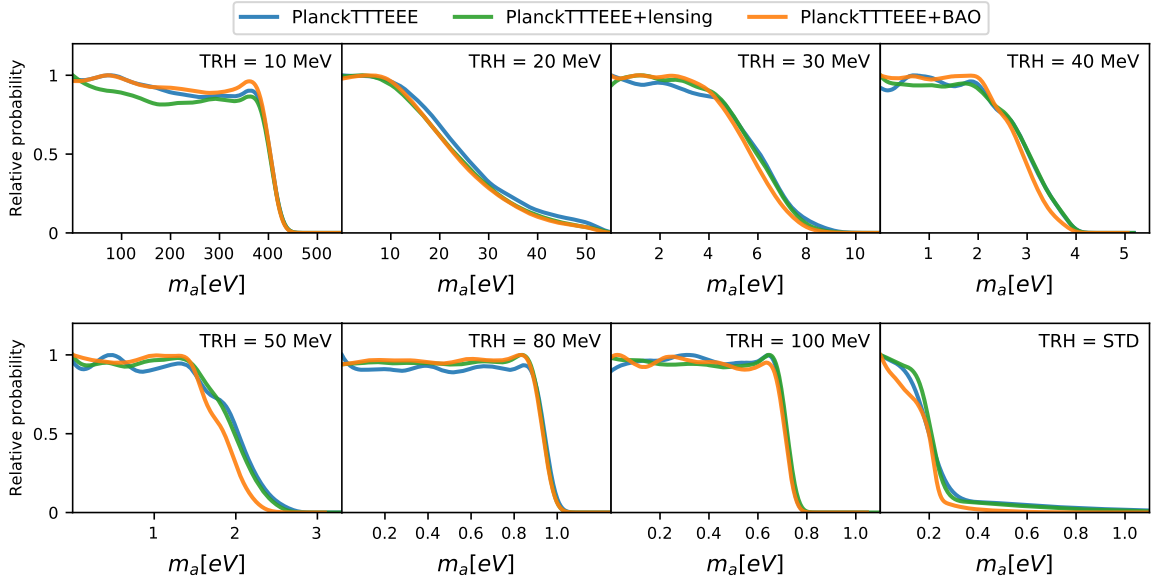


Figure 6. Posterior probability distributions for m_a for different values of the reheating temperature T_{RH} . We show constraints from PlanckTTTEEE alone (blue) and in combination with Planck lensing (green) or BAO data (orange). Each posterior is normalized to its maximum and has been smoothed using a Gaussian kernel with width equal to 0.2 standard deviations of the distribution.

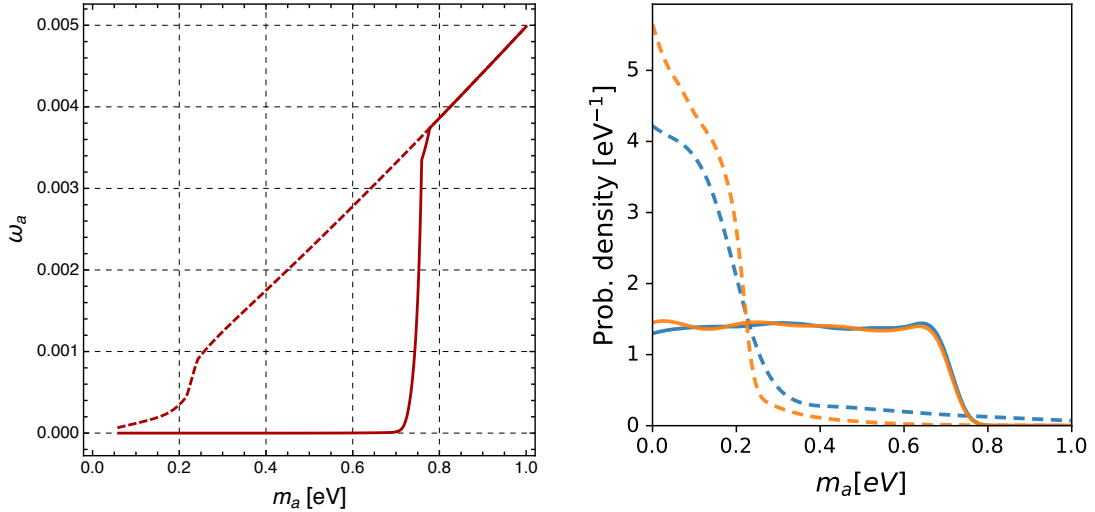


Figure 7. Left panel: axion density parameter ω_a as a function of the axion mass, for $T_{\text{RH}} = 100$ MeV (solid) and for the standard thermal history (dashed). Right panel: Posterior probability distributions for $T_{\text{RH}} = 100$ MeV (solid) and for the standard thermal history (dashed). We show constraints from PlanckTTTEEE alone (blue) and in combination with BAO data (orange). Contrarily to Fig. 6, here the posteriors are normalized so that they integrate to unity, to better appreciate the difference in the probability densities.

increase with the reheating temperature (see Fig. 2), and this explains why the improve-

ments become increasingly smaller and eventually vanish with larger T_{RH} . On the contrary, inclusion of lensing and BAO data significantly improves the constraints on the axion mass in the standard scenario: we obtain $m_a < 0.84, 0.64, 0.26$ eV for PlanckTTTEEE, Planck-TTTEEE+lensing and PlanckTTTEEE+BAO, respectively. This improvements reflect the fact that, for the standard thermal history, the axion density varies relatively smoothly with their mass. Let us finally note that the observed dependence of the constraints from the dataset used is in agreement with the fact that the density of massive light relics is better constrained by adding current BAO information, rather than the measurements of the reconstructed lensing potential, to the Planck observations of temperature and polarization anisotropies.

We remark that our mass bounds in low-reheating temperature scenarios represent a significant improvement with respect to the seminal paper GSK08 [42]. For the largest value of the reheating temperature considered here, $T_{\text{RH}} \lesssim 100$ MeV, GSK08 find $m_a \lesssim 2$ eV at 95% C.L., as it can be inferred from a visual inspection of their Fig. 1. Our bound $m_a \lesssim 0.7$ eV thus represents a factor three improvement with respect to that result. However, the most striking improvement is found for low values of the reheating temperature. Indeed, in GSK08 it was found that the LSS/CMB bounds obtained from WMAP1/SDSS data, and based on free-streaming arguments, are completely lifted for $T_{\text{RH}} \lesssim 35$ MeV. Below that value of the reheating temperature, bounds were obtained from the looser requirement that the axion density does not exceed the total dark matter density, as also discussed here in Sec. 3. Given the precision of the data used in our analysis, we find that the lowest reheating temperature for which free streaming plays a role in determining constraints is lowered, lying somewhere in the 10 – 20 MeV range, as discussed in the previous sections. In GSK08, it is found that the free-streaming argument excludes masses larger than 20 eV for $T_{\text{RH}} \simeq 35$ MeV, while the total density constraint yields $m_a < 200$ eV for $T_{\text{RH}} \simeq 20$ MeV. For comparison, in the present analysis we have found that $m_a \lesssim 5$ eV for $T_{\text{RH}} \simeq 35$ MeV, and $m_a \lesssim 20$ eV for $T_{\text{RH}} \simeq 20$ MeV. We stress again that, in our case, free streaming still plays a role in determining the constrain at $T_{\text{RH}} \simeq 20$ MeV.

We comment that for masses $m_a > 18$ eV the axion lifetime with respect to radiative decay would be shorter than the lifetime of the Universe [87], unless the axion-photon coupling is suppressed [71]. Therefore, our analysis might not apply in this regime. Note that axion decay might lead to other cosmological signatures, like e.g. changes in the ionization history of the Universe in the case of radiative decays [88]. Radiative decays of axions with masses of few eV might also affect the extra-galactic background light [89–92]. Given the bounds shown in Table 1, this means that for $T_{\text{RH}} < 30$ MeV the mass of axions stable on cosmological timescales is essentially unconstrained by the data considered in this analysis.

As mentioned above, we also note that it was recently suggested [74] that the chiral expansion effective field theory, upon which the computation of the axion-pion thermalization rate is based, might fail at temperatures larger than $T_\chi \simeq 62$ MeV. This would make the computation of the relic abundance of axions unreliable for the smaller masses that yield $T_D > T_\chi$. For the standard thermal history, this corresponds to $m_a \lesssim 1.1$ eV. We have computed the mass $m_{a,\chi}$ that yields $T_D = T_\chi$ for the reheating temperatures in consideration; these are shown in Tab. 2. We see that the allowed regions that we find for $T_{\text{RH}} \geq 50$ MeV from the most constraining dataset, PlanckTTTEEE+BAO, fall completely within the region in which the validity of the chiral expansion has been questioned.

We summarize our findings in Fig. 8, where we show the bounds on the axion mass from Planck temperature and polarization measurements in combination with BAO data, as

$T_{\text{RH}} [\text{MeV}]$	$m_{a,\chi} [\text{eV}]$
10	12
20	6.0
30	3.9
40	2.9
50	2.3
80	1.1
100	1.1
∞	1.1

Table 2. Axion mass $m_{a,\chi}$ corresponding to a decoupling temperature T_D equal to $T_\chi = 62 \text{ MeV}$, for different values of the reheating temperature T_{RH} . The standard computation of the axion thermalization rate has been suggested to be unreliable at $T > T_\chi$ [74]. Axion with masses $m_a < m_{a,\chi}$ would decouple, according to the standard calculation, at $T_D > T_\chi$.

a function of the reheating temperature. Even taking into account the finite lifetime of high-mass axions and the possible failure of chiral effective field theory in the small mass regime, our analysis shows that masses in the 3 – 20 eV range are allowed for sufficiently low values ($T_{\text{RH}} \leq 40 \text{ MeV}$) of the reheating temperature. For values of the reheating temperature larger than 50 MeV, instead, we find that all values of the mass for which the decoupling happens within the range of validity of the chiral EFT suggested by Ref. [74] are excluded by the data.

6 Conclusions

We have re-examined cosmological bounds on thermal axions based on the 2018 CMB temperature anisotropy measurement provided by the Planck mission, as well as other types of cosmological observations. In the case of standard cosmological scenario we find an axion mass bound $m_a < 0.259 \text{ eV}$, comparable with the one recently placed in Ref. [19] using a similar dataset. Our main goal has been to analyze how this bound would change in cosmological models with a low-reheating temperature T_{RH} . We find that for $T_{\text{RH}} \lesssim 80 \text{ MeV}$ the bound would relax to $m_a \lesssim \mathcal{O}(1) \text{ eV}$, becoming looser than $m_a \lesssim 10 \text{ eV}$ for $T_{\text{RH}} \lesssim 30 \text{ MeV}$. We remark that these reheating temperatures are still sufficiently high to leave unperturbed the neutrino thermalization [31, 32]. Therefore, axions would represent the only thermal relics sensitive to a range of reheating temperatures greater than the one probed by neutrinos ($T_{\text{RH}} \sim 5 \text{ MeV}$).

Our result together with the recent one presented in [74] questions the range of validity of the cosmological mass bound on axions. In [74] it has been shown that for $m_a \lesssim 1 \text{ eV}$ the bound is not reliable since it is obtained by extrapolating the chiral expansion in a region where the effective field theory breaks down. Furthermore, we have shown that the bound is model dependent and would be significantly relaxed in non-standard cosmologies, in a region in which other cosmological observables would not be affected. Therefore, multi-eV axions do not seem necessarily excluded by cosmology alone. This finding would motivate the necessity to come back to the astrophysical arguments in order to assess the robustness of the constraints for multi-eV axions. In particular, recent analyses seem to disfavor axions in this mass range from the supernova cooling [64]. Our results would motivate a dedicated supernova simulation including multi-eV axions to definitely clarify this issue.

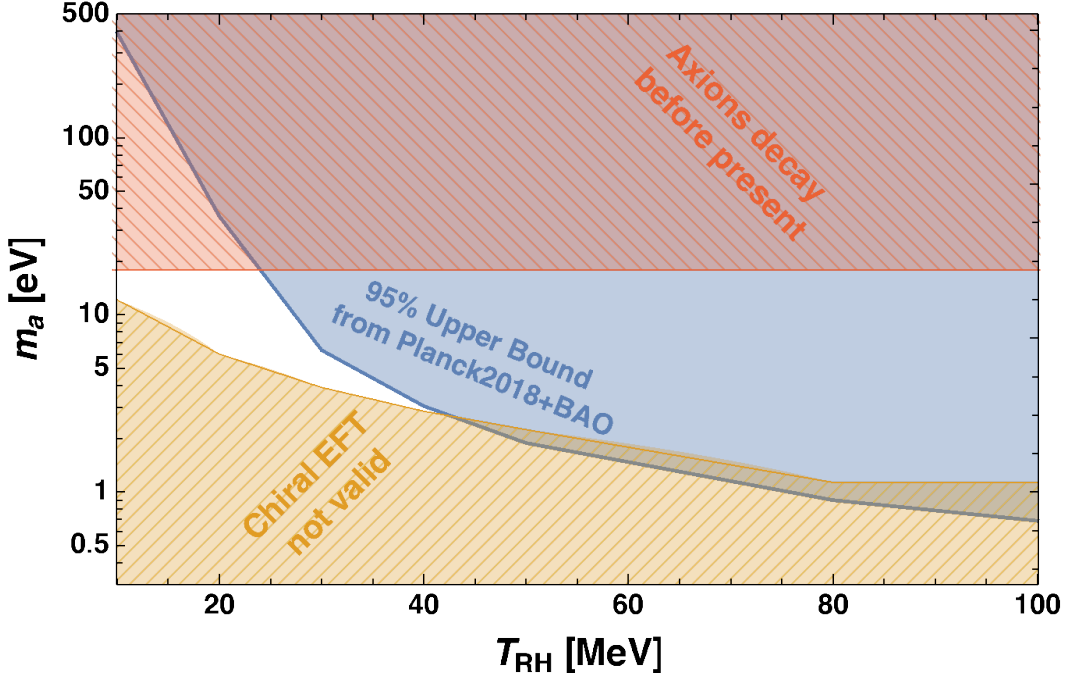


Figure 8. Upper bounds on the axion mass as a function of the reheating temperature (solid blue line). The shaded blue area is excluded by our analysis, that neglects axion decays and assumes validity of the chiral effective field theory. The hatched areas mark the regions where i) the axion lifetime is larger than the present age of the Universe (red) (unless the axion photon coupling is suppressed), or ii) the computation of the axion-pion decay rate might fail (yellow, see text for discussion), and as such our analysis might not apply.

We remark that cosmological bounds on thermal axions are important in relation to direct search of axions at helioscope experiments [20, 93]. In particular, the CERN Axion Solar Telescope (CAST) in their search for solar axions in the phase with ^3He buffer gas, has reached a mass $m_a < 1.17$ eV [93]. However, CAST cannot detect larger masses due to the loss of coherence of axion-photon conversions in the magnetic field of the detector. Also the future axion helioscope IAXO is not expected to reach a larger mass range. In this sense, the axion mass bound in the standard cosmological case is nicely complementary to the sensitivity of helioscopes search. Notably, it would allow to cover all the axion mass region around the eV without any gap. Our result shows that the cosmological bound is model-dependent and can be significantly loosened in presence of low-reheating temperatures, which leave undisturbed the neutrino sector. Therefore, it seems mandatory to assess new experimental strategies to probe multi-eV axions. In this regard, there are ideas for a new class of helioscopes, like the proposed AMELIE (An Axion Modulation hELioscope Experiment), which could be sensitive to axions with masses from a few meV to several eV, thanks to the use of a Time Projection Chamber [94]. Studies for low mass WIMPs are already being carried out by the TREX-DM experiment [95, 96], which is taking data at the Canfranc Underground Laboratory (LSC) [97]. The project aims at demonstrating the feasibility to reach low backgrounds at low energy thresholds for dark matter searches, which require similar detection conditions as for axions. Furthermore, axions with mass $m_a \lesssim 100$ eV could be detected with a dark matter detector like the Cryogenic Underground Observatory for Rare Events (CUORE),

which exploits the inverse Bragg-Primakoff effect to detect solar axions [98–100]. It is also intriguing to mention that multi-eV would lead to an enhancement in the solar axion flux via resonant production in the solar magnetic field [101]. Furthermore, axions with masses between 2-3 eV decaying into photons might explain the measured excess in the infrared photon background [89–92]. From a model-building perspective, there exist “astrophobic” models in which one would relax the axion mass bounds above eV [102]. Furthermore, models have been conceived to accomodate together both hadronic axions and sterile neutrinos [103, 104]. In this context, it has been recently proposed that low-reheating scenarios would reconcile eV-sterile neutrinos with cosmological observations [33] (see also [105–107] for a study of the impact of low-reheating scenarios on heavy sterile neutrinos). So if hints of eV-sterile neutrinos would be confirmed, they would strengthen the case for low-reheating scenarios and for multi-eV axions.

New detection possibilities need to be put on the agenda of the experimental strategies for axions, in order to explore the multi-eV mass region where surprises might emerge. Indeed, if multi-eV axion should be found by one of these experiments, this would be unavoidably in tension with standard cosmological bound. Therefore, such a discovery would be not only revolutionary for particle physics, but would also produce a radical change in our description of the cosmological evolution of the Universe.

Acknowledgments

We warmly thank Maurizio Giannotti, Steen Hannestad and Georg Raffelt for useful comments on our manuscript, and Martina Gerbino for useful discussions. The work of P.C. and A.M. is partially supported by the Italian Istituto Nazionale di Fisica Nucleare (INFN) through the “Theoretical Astroparticle Physics” project and by the research grant number 2017W4HA7S “NAT-NET: Neutrino and Astroparticle Theory Network” under the program PRIN 2017 funded by the Italian Ministero dell’Università e della Ricerca (MUR). M.L. and F.F. acknowledge support from the COSMOS network (www.cosmosnet.it) through the ASI (Italian Space Agency) Grants 2016-24-H.0, 2016-24-H.1-2018 and 2019-9-HH.0. We acknowledge the use of computing facilities provided by the INFN theory group (I.S. InDark) at CINECA.

Appendix: Axion decoupling in low-temperature reheating scenario

In this Appendix we provide more details on axion thermalization in the low-temperature reheating scenario, closely following the discussion given in [42]. The radiation-dominated era of the Universe might be originated by the decay of a scalar field, that dominated the Universe until the decay. The process of decay of a scalar field and thermalization of the produced particles is called reheating. In the history of the Universe one cannot exclude that the reheating phenomenon happened more than once. From a phenomenological point of view, we are interested only in the last reheating before the primordial nucleosynthesis. The field responsible for the reheating is usually associated with the inflaton and the temperature at which reheating occurs is denoted with T_{RH} . Observations cannot exclude reheating temperatures as low as 1 MeV, and these models are called Low-Temperature Reheating scenarios. We suppose an initial phase dominated by a non-relativistic scalar field ϕ (for simplicity we call it inflaton), whose decay produces radiation that dominates the second phase. At the beginning of reheating the Hubble parameter is determined entirely by the

energy density of the inflaton

$$H_0^2 = \frac{8\pi}{3m_P^2} \rho_{0,\phi} ; \quad (6.1)$$

and the Boltzmann equations for the inflaton and radiation energy densities are

$$\begin{aligned} \dot{\rho}_\phi + 3H\rho_\phi &= -\Gamma_\phi \rho_\phi , \\ \dot{\rho}_R + 4H\rho_R &= \Gamma_\phi \rho_\phi ; \end{aligned} \quad (6.2)$$

assuming a constant inflaton decay rate Γ_ϕ . The two energy densities scale as radiation and non-relativistic matter. Then $\rho_\phi \sim a^{-3}e^{-\Gamma t}$, where the decay factor accounts for the inflaton decay. At the beginning of the reheating this term can be neglected and the radiation has an energy density

$$\rho_R = \Gamma \rho_{0,\phi} t_0 \frac{3}{5} \left[\left(\frac{a_0}{a} \right)^{3/2} - \left(\frac{a_0}{a} \right)^4 \right] ; \quad (6.3)$$

where a_0 is the scale factor at the beginning of reheating and it is easy to see that the maximum radiation density is achieved for $a_m = a_0(8/3)^{2/5}$. Much later than a_0 , the radiation density is proportional to $a^{-3/2}$. The temperature T_{RH} at which reheating is completed is given by

$$H^2 = \Gamma_\phi^2 = \frac{8\pi}{3m_P^2} \frac{\pi^2}{30} g_{*,RH} T_{RH}^4 ; \quad (6.4)$$

where $g_{*,RH} = g_*(T_{RH})$ is the effective number of thermal degrees of freedom.

During the reheating phase, the temperature scales as

$$T = \left(\frac{30}{\pi^2 g_*(T)} \rho_R \right)^{1/4} = T_m \left(\frac{g_*(T_m)}{g_*(T)} \right)^{1/4} \left(\frac{a_m}{a} \right)^{3/8} ; \quad (6.5)$$

where $T_m = T(a_m)$. Thanks to the results above, one obtains the following Hubble parameter during reheating

$$H = \left[\frac{5}{9} \pi^3 \frac{g_*(T)^2}{g_*(T_{RH})} \right]^{1/2} \frac{T^4}{T_{RH}^2 m_P} ; \quad (6.6)$$

that can be compared with the standard scenario

$$H = \sqrt{\frac{4\pi^3}{45} g_*(T)} \frac{T^2}{m_P} . \quad (6.7)$$

Therefore, during reheating, the Universe expands faster than the standard scenario as can be seen from Fig. 9, where the jump in the behavior at $T = 150$ MeV is due to the increase of the thermal degrees of freedom after the QCD phase transitions.

The axion density at the decoupling $n_{a,D}$ is diluted by the adiabatic Universe expansion as

$$\Omega_a = \frac{n_{a,D} m_a}{\rho_c} \begin{cases} \left(\frac{a_D}{a_0} \right)^3 & \text{for } T_D < T_{RH} \\ \left(\frac{a_D}{a_{RH}} \right)^3 \left(\frac{a_{RH}}{a_0} \right)^3 & \text{for } T_D \geq T_{RH} ; \end{cases} \quad (6.8)$$

where $\rho_c = 1.05 \times 10^4 h^2 \text{ eV cm}^{-3}$ is the critical density of the Universe. The scale factor during the standard phase scales as

$$\left(\frac{a_{RH}}{a} \right)^3 = \left(\frac{T}{T_{RH}} \right)^3 \frac{g_{*,S}(T)}{g_{*,S}(T_{RH})} ; \quad (6.9)$$

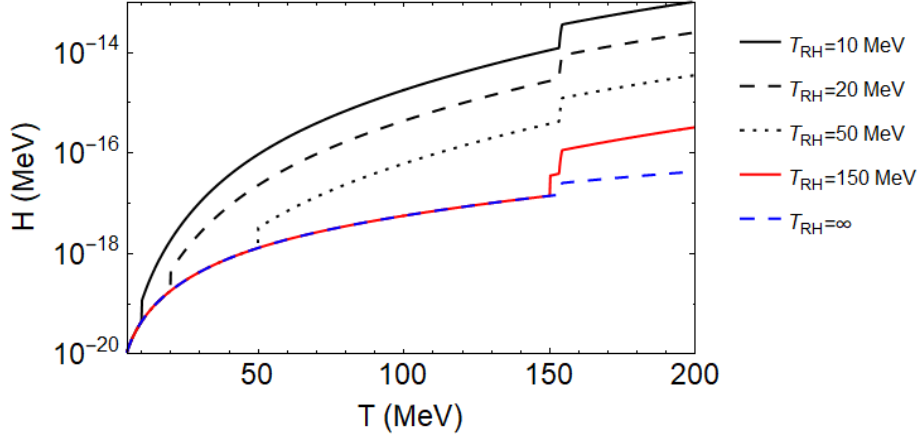


Figure 9. Evolution with temperature of the Hubble parameter, for different reheating temperatures T_{RH} .

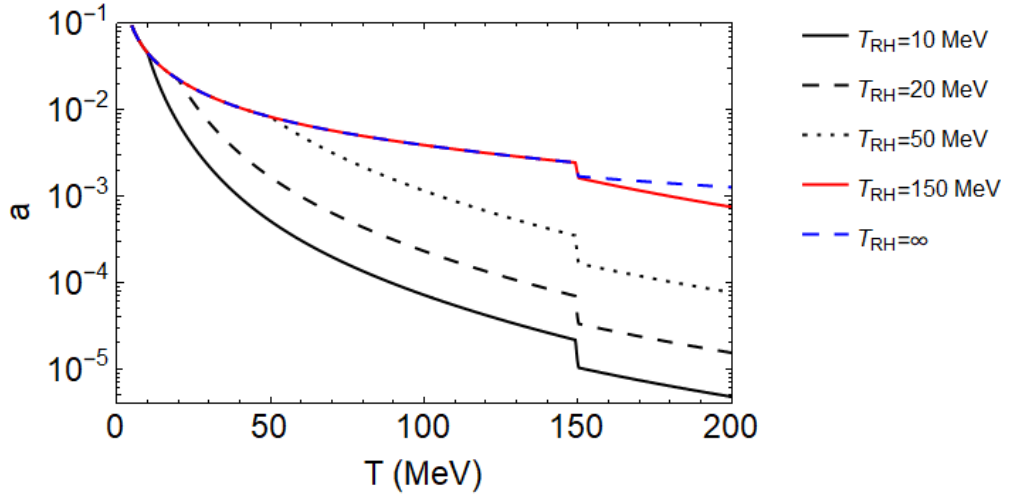


Figure 10. Scale factor for different reheating temperatures T_{RH} .

and during the reheating phase as

$$\left(\frac{a_D}{a_{RH}}\right)^3 = \left(\frac{T_{RH}}{T_D}\right)^8 \left[\frac{g_*(T_{RH})}{g_*(T_D)}\right]^2; \quad (6.10)$$

where the behaviour of these scale factors is given in Fig. 10.

Thus, from Eq. (6.8) the axion abundance is

$$\Omega_a h^2 = \frac{m_a}{13 \text{ eV}} \frac{1}{g_{*,S}(T_D)} \begin{cases} 1 & \text{for } T_D < T_{RH} \\ \left(\frac{T_{RH}}{T_D}\right)^5 \left[\frac{g_*(T_{RH})}{g_*(T_D)}\right]^2 \left[\frac{g_{*,S}(T_D)}{g_{*,S}(T_{RH})}\right] & \text{for } T_D \geq T_{RH}; \end{cases} \quad (6.11)$$

the extra factor suppresses the relic abundance if $T_{RH} < T_D$. In the standard scenario this term is equal to one. Note that this result does not depend on the initial value of the Hubble parameter H_0 or the maximum temperature T_m . An extra axion component in the radiation

fluid, as long as it is ultrarelativistic, leads to an increase of the effective number of relativistic degrees of freedom

$$N_{\text{eff}} = 3 + \left(\frac{\rho_a}{\rho_\gamma}\right) \left(\frac{8}{7}\right) \left(\frac{11}{4}\right)^{4/3} ; \quad (6.12)$$

where ρ_a and ρ_γ are the axion and photon energy densities, respectively. This deviation is quantified by

$$\Delta N_{\text{eff}} = \left(\frac{4}{7}\right) \left(\frac{11}{4}\right)^{4/3} \left(\frac{T_D}{T}\right)^4 \begin{cases} \left(\frac{T}{T_{\text{RH}}}\right)^4 \left[\frac{g_{*,S}(T)}{g_{*,S}(T_{\text{RH}})}\right]^{4/3} & \text{for } T_D < T_{\text{RH}} \\ \left(\frac{T_{\text{RH}}}{T_D}\right)^{32/3} \left[\frac{g_{*,S}(T_{\text{RH}})}{g_{*,S}(T_D)}\right]^{8/3} \left(\frac{T}{T_{\text{RH}}}\right)^4 \left[\frac{g_{*,S}(T)}{g_{*,S}(T_{\text{RH}})}\right]^{4/3} & \text{for } T_D \geq T_{\text{RH}} ; \end{cases} \quad (6.13)$$

where we used the scaling relations in Eqs. (6.9)-(6.10). Similar relations hold for the axion-to-photon temperature ratio, properly rescaling the axion decoupling temperature to account for the different cosmological phases

$$\mathcal{T}_a = \frac{T_a}{T} = \frac{T_D}{T} \frac{a_D}{a} = \begin{cases} \left[\frac{g_{*,S}(T)}{g_{*,S}(T_D)}\right]^{1/3} & \text{for } T_D < T_{\text{RH}} \\ \left[\frac{g_{*,S}(T)}{g_{*,S}(T_{\text{RH}})}\right]^{1/3} \left(\frac{T_{\text{RH}}}{T_D}\right)^{5/3} \left[\frac{g_{*,S}(T_{\text{RH}})}{g_{*,S}(T_D)}\right]^{2/3} & \text{for } T_D \geq T_{\text{RH}} . \end{cases} \quad (6.14)$$

Finally, the momentum-to-mass ratio is defined as

$$\frac{\langle p_a \rangle}{m_a} = \frac{2.7 T_a}{m_a} = \frac{2.7 T}{m_a} \mathcal{T}_a , \quad (6.15)$$

where $T = T_{\text{today}}(1+z)$ and we have calculated the average momentum by mediating over a Bose-Einstein distribution.

References

- [1] J. Lesgourgues and S. Pastor, *Massive neutrinos and cosmology*, *Phys. Rept.* **429** (2006) 307 [[astro-ph/0603494](#)].
- [2] J. Lesgourgues and S. Pastor, *Neutrino cosmology and Planck*, *New J. Phys.* **16** (2014) 065002 [[1404.1740](#)].
- [3] M. Archidiacono, E. Giusarma, S. Hannestad and O. Mena, *Cosmic dark radiation and neutrinos*, *Adv. High Energy Phys.* **2013** (2013) 191047 [[1307.0637](#)].
- [4] F. Capozzi, E. Di Valentino, E. Lisi, A. Marrone, A. Melchiorri and A. Palazzo, *Global constraints on absolute neutrino masses and their ordering*, *Phys. Rev. D* **95** (2017) 096014 [[2003.08511](#)]. [Addendum: *Phys.Rev.D* 101, 116013 (2020)].
- [5] M. Lattanzi and M. Gerbino, *Status of neutrino properties and future prospects - Cosmological and astrophysical constraints*, *Front. in Phys.* **5** (2018) 70 [[1712.07109](#)].
- [6] S. Roy Choudhury and S. Hannestad, *Updated results on neutrino mass and mass hierarchy from cosmology with Planck 2018 likelihoods*, *JCAP* **07** (2020) 037 [[1907.12598](#)].
- [7] S. Hannestad and G. Raffelt, *Cosmological mass limits on neutrinos, axions, and other light particles*, *JCAP* **04** (2004) 008 [[hep-ph/0312154](#)].
- [8] S. Hannestad, A. Mirizzi and G. Raffelt, *New cosmological mass limit on thermal relic axions*, *JCAP* **07** (2005) 002 [[hep-ph/0504059](#)].

- [9] A. Melchiorri, O. Mena and A. Slosar, *An improved cosmological bound on the thermal axion mass*, *Phys. Rev. D* **76** (2007) 041303 [[0705.2695](#)].
- [10] S. Hannestad, A. Mirizzi, G. G. Raffelt and Y. Y. Y. Wong, *Cosmological constraints on neutrino plus axion hot dark matter*, *JCAP* **08** (2007) 015 [[0706.4198](#)].
- [11] S. Hannestad, A. Mirizzi, G. G. Raffelt and Y. Y. Y. Wong, *Neutrino and axion hot dark matter bounds after WMAP-7*, *JCAP* **08** (2010) 001 [[1004.0695](#)].
- [12] E. Giusarma, E. Di Valentino, M. Lattanzi, A. Melchiorri and O. Mena, *Relic Neutrinos, thermal axions and cosmology in early 2014*, *Phys. Rev. D* **90** (2014) 043507 [[1403.4852](#)].
- [13] E. Di Valentino, E. Giusarma, M. Lattanzi, O. Mena, A. Melchiorri and J. Silk, *Cosmological Axion and neutrino mass constraints from Planck 2015 temperature and polarization data*, *Phys. Lett. B* **752** (2016) 182 [[1507.08665](#)].
- [14] M. Archidiacono, S. Hannestad, A. Mirizzi, G. Raffelt and Y. Y. Y. Wong, *Axion hot dark matter bounds after Planck*, *JCAP* **10** (2013) 020 [[1307.0615](#)].
- [15] M. Archidiacono, T. Basse, J. Hamann, S. Hannestad, G. Raffelt and Y. Y. Y. Wong, *Future cosmological sensitivity for hot dark matter axions*, *JCAP* **05** (2015) 050 [[1502.03325](#)].
- [16] E. Di Valentino, S. Gariazzo, E. Giusarma and O. Mena, *Robustness of cosmological axion mass limits*, *Phys. Rev. D* **91** (2015) 123505 [[1503.00911](#)].
- [17] J. E. Kim, *Weak Interaction Singlet and Strong CP Invariance*, *Phys. Rev. Lett.* **43** (1979) 103.
- [18] M. A. Shifman, A. I. Vainshtein and V. I. Zakharov, *Can Confinement Ensure Natural CP Invariance of Strong Interactions?*, *Nucl. Phys. B* **166** (1980) 493.
- [19] W. Giarè, E. Di Valentino, A. Melchiorri and O. Mena, *New cosmological bounds on hot relics: Axions & Neutrinos*, [2011.14704](#).
- [20] IAXO Collaboration, E. Armengaud et al., *Physics potential of the International Axion Observatory (IAOX)*, *JCAP* **06** (2019) 047 [[1904.09155](#)].
- [21] M. Dine, W. Fischler and M. Srednicki, *A Simple Solution to the Strong CP Problem with a Harmless Axion*, *Phys. Lett. B* **104** (1981) 199.
- [22] A. R. Zhitnitsky, *On Possible Suppression of the Axion Hadron Interactions. (In Russian)*, *Sov. J. Nucl. Phys.* **31** (1980) 260.
- [23] R. Z. Ferreira, A. Notari and F. Rompineve, *Dine-Fischler-Srednicki-Zhitnitsky axion in the CMB*, *Phys. Rev. D* **103** (2021) 063524 [[2012.06566](#)].
- [24] D. Baumann, D. Green and B. Wallisch, *New Target for Cosmic Axion Searches*, *Phys. Rev. Lett.* **117** (2016) 171301 [[1604.08614](#)].
- [25] CMB-S4 Collaboration, K. N. Abazajian et al., *CMB-S4 Science Book, First Edition*, [1610.02743](#).
- [26] R. Z. Ferreira and A. Notari, *Observable Windows for the QCD Axion Through the Number of Relativistic Species*, *Phys. Rev. Lett.* **120** (2018) 191301 [[1801.06090](#)].
- [27] I. G. Irastorza and J. Redondo, *New experimental approaches in the search for axion-like particles*, *Prog. Part. Nucl. Phys.* **102** (2018) 89 [[1801.08127](#)].
- [28] M. Kawasaki, K. Kohri and N. Sugiyama, *MeV scale reheating temperature and thermalization of neutrino background*, *Phys. Rev. D* **62** (2000) 023506 [[astro-ph/0002127](#)].
- [29] S. Hannestad, *What is the lowest possible reheating temperature?*, *Phys. Rev. D* **70** (2004) 043506 [[astro-ph/0403291](#)].
- [30] K. Ichikawa, M. Kawasaki and F. Takahashi, *The Oscillation effects on thermalization of the*

neutrinos in the Universe with low reheating temperature, *Phys. Rev. D* **72** (2005) 043522 [[astro-ph/0505395](#)].

- [31] P. F. de Salas, M. Lattanzi, G. Mangano, G. Miele, S. Pastor and O. Pisanti, *Bounds on very low reheating scenarios after Planck*, *Phys. Rev. D* **92** (2015) 123534 [[1511.00672](#)].
- [32] T. Hasegawa, N. Hiroshima, K. Kohri, R. S. L. Hansen, T. Tram and S. Hannestad, *MeV-scale reheating temperature and thermalization of oscillating neutrinos by radiative and hadronic decays of massive particles*, *JCAP* **12** (2019) 012 [[1908.10189](#)].
- [33] T. Hasegawa, N. Hiroshima, K. Kohri, R. S. L. Hansen, T. Tram and S. Hannestad, *MeV-scale reheating temperature and cosmological production of light sterile neutrinos*, *JCAP* **08** (2020) 015 [[2003.13302](#)].
- [34] D. J. H. Chung, E. W. Kolb and A. Riotto, *Production of massive particles during reheating*, *Phys. Rev. D* **60** (1999) 063504 [[hep-ph/9809453](#)].
- [35] E. W. Kolb, A. Notari and A. Riotto, *On the reheating stage after inflation*, *Phys. Rev. D* **68** (2003) 123505 [[hep-ph/0307241](#)].
- [36] G. N. Felder, L. Kofman and A. D. Linde, *Gravitational particle production and the moduli problem*, *JHEP* **02** (2000) 027 [[hep-ph/9909508](#)].
- [37] G. F. Giudice, E. W. Kolb and A. Riotto, *Largest temperature of the radiation era and its cosmological implications*, *Phys. Rev. D* **64** (2001) 023508 [[hep-ph/0005123](#)].
- [38] L. Visinelli and J. Redondo, *Axion Miniclusters in Modified Cosmological Histories*, *Phys. Rev. D* **101** (2020) 023008 [[1808.01879](#)].
- [39] N. Blinov, M. J. Dolan, P. Draper and J. Kozaczuk, *Dark matter targets for axionlike particle searches*, *Phys. Rev. D* **100** (2019) 015049 [[1905.06952](#)].
- [40] N. Blinov, M. J. Dolan and P. Draper, *Imprints of the Early Universe on Axion Dark Matter Substructure*, *Phys. Rev. D* **101** (2020) 035002 [[1911.07853](#)].
- [41] N. Ramberg and L. Visinelli, *Probing the Early Universe with Axion Physics and Gravitational Waves*, *Phys. Rev. D* **99** (2019) 123513 [[1904.05707](#)].
- [42] D. Grin, T. L. Smith and M. Kamionkowski, *Axion constraints in non-standard thermal histories*, *Phys. Rev. D* **77** (2008) 085020 [[0711.1352](#)].
- [43] R. D. Peccei and H. R. Quinn, *CP Conservation in the Presence of Instantons*, *Phys. Rev. Lett.* **38** (1977) 1440.
- [44] R. D. Peccei and H. R. Quinn, *Constraints Imposed by CP Conservation in the Presence of Instantons*, *Phys. Rev. D* **16** (1977) 1791.
- [45] S. Weinberg, *A New Light Boson?*, *Phys. Rev. Lett.* **40** (1978) 223.
- [46] F. Wilczek, *Problem of Strong P and T Invariance in the Presence of Instantons*, *Phys. Rev. Lett.* **40** (1978) 279.
- [47] G. Grilli di Cortona, E. Hardy, J. Pardo Vega and G. Villadoro, *The QCD axion, precisely*, *JHEP* **01** (2016) 034 [[1511.02867](#)].
- [48] S. Borsanyi et al., *Calculation of the axion mass based on high-temperature lattice quantum chromodynamics*, *Nature* **539** (2016) 69 [[1606.07494](#)].
- [49] PARTICLE DATA GROUP Collaboration, M. Tanabashi et al., *Review of Particle Physics*, *Phys. Rev. D* **98** (2018) 030001.
- [50] M. Giannotti, I. G. Irastorza, J. Redondo, A. Ringwald and K. Saikawa, *Stellar Recipes for Axion Hunters*, *JCAP* **10** (2017) 010 [[1708.02111](#)].
- [51] J. Preskill, M. B. Wise and F. Wilczek, *Cosmology of the Invisible Axion*, *Phys. Lett. B* **120**

(1983) 127.

- [52] M. Dine and W. Fischler, *The Not So Harmless Axion*, *Phys. Lett. B* **120** (1983) 137.
- [53] L. F. Abbott and P. Sikivie, *A Cosmological Bound on the Invisible Axion*, *Phys. Lett. B* **120** (1983) 133.
- [54] P. Sikivie, *Axion Cosmology*, *Lect. Notes Phys.* **741** (2008) 19 [[astro-ph/0610440](#)].
- [55] ADMX Collaboration, N. Du et al., *A Search for Invisible Axion Dark Matter with the Axion Dark Matter Experiment*, *Phys. Rev. Lett.* **120** (2018) 151301 [[1804.05750](#)].
- [56] ADMX Collaboration, T. Braine et al., *Extended Search for the Invisible Axion with the Axion Dark Matter Experiment*, *Phys. Rev. Lett.* **124** (2020) 101303 [[1910.08638](#)].
- [57] MADMAX WORKING GROUP Collaboration, A. Caldwell, G. Dvali, B. Majorovits, A. Millar, G. Raffelt, J. Redondo, O. Reimann, F. Simon and F. Steffen, *Dielectric Haloscopes: A New Way to Detect Axion Dark Matter*, *Phys. Rev. Lett.* **118** (2017) 091801 [[1611.05865](#)].
- [58] E. Masso, F. Rota and G. Zsembinski, *On axion thermalization in the early universe*, *Phys. Rev. D* **66** (2002) 023004 [[hep-ph/0203221](#)].
- [59] P. Graf and F. D. Steffen, *Thermal axion production in the primordial quark-gluon plasma*, *Phys. Rev. D* **83** (2011) 075011 [[1008.4528](#)].
- [60] A. Salvio, A. Strumia and W. Xue, *Thermal axion production*, *JCAP* **01** (2014) 011 [[1310.6982](#)].
- [61] T. Moroi and H. Murayama, *Axionic hot dark matter in the hadronic axion window*, *Phys. Lett. B* **440** (1998) 69 [[hep-ph/9804291](#)].
- [62] S. Chang and K. Choi, *Hadronic axion window and the big bang nucleosynthesis*, *Phys. Lett. B* **316** (1993) 51 [[hep-ph/9306216](#)].
- [63] G. G. Raffelt, *Astrophysical axion bounds*, *Lect. Notes Phys.* **741** (2008) 51 [[hep-ph/0611350](#)].
- [64] P. Carenza, T. Fischer, M. Giannotti, G. Guo, G. Martínez-Pinedo and A. Mirizzi, *Improved axion emissivity from a supernova via nucleon-nucleon bremsstrahlung*, *JCAP* **10** (2019) 016 [[1906.11844](#)]. [Erratum: JCAP 05, E01 (2020)].
- [65] P. Carenza, B. Fore, M. Giannotti, A. Mirizzi and S. Reddy, *Enhanced Supernova Axion Emission and its Implications*, *Phys. Rev. Lett.* **126** (2021) 071102 [[2010.02943](#)].
- [66] L. Di Luzio, M. Giannotti, E. Nardi and L. Visinelli, *The landscape of QCD axion models*, *Phys. Rept.* **870** (2020) 1 [[2003.01100](#)].
- [67] F. Capozzi and G. Raffelt, *Axion and neutrino bounds improved with new calibrations of the tip of the red-giant branch using geometric distance determinations*, *Phys. Rev. D* **102** (2020) 083007 [[2007.03694](#)].
- [68] O. Straniero, C. Pallanca, E. Dalessandro, I. Dominguez, F. R. Ferraro, M. Giannotti, A. Mirizzi and L. Piersanti, *The RGB tip of galactic globular clusters and the revision of the axion-electron coupling bound*, *Astron. Astrophys.* **644** (2020) A166 [[2010.03833](#)].
- [69] A. Ayala, I. Domínguez, M. Giannotti, A. Mirizzi and O. Straniero, *Revisiting the bound on axion-photon coupling from Globular Clusters*, *Phys. Rev. Lett.* **113** (2014) 191302 [[1406.6053](#)].
- [70] O. Straniero, A. Ayala, M. Giannotti, A. Mirizzi and I. Dominguez, *Axion-Photon Coupling: Astrophysical Constraints*, in *11th Patras Workshop on Axions, WIMPs and WISPs*, 2015, DOI.
- [71] D. B. Kaplan, *Opening the Axion Window*, *Nucl. Phys. B* **260** (1985) 215.
- [72] P. Di Vecchia and G. Veneziano, *Chiral Dynamics in the Large n Limit*, *Nucl. Phys. B* **171**

(1980) 253.

- [73] H. Georgi, D. B. Kaplan and L. Randall, *Manifesting the Invisible Axion at Low-energies*, *Phys. Lett. B* **169** (1986) 73.
- [74] L. Di Luzio, G. Martinelli and G. Piazza, *Axion hot dark matter bound, reliably*, [2101.10330](#).
- [75] L. Husdal, *On Effective Degrees of Freedom in the Early Universe*, *Galaxies* **4** (2016) 78 [[1609.04979](#)].
- [76] PLANCK Collaboration, N. Aghanim et al., *Planck 2018 results. VI. Cosmological parameters*, *Astron. Astrophys.* **641** (2020) A6 [[1807.06209](#)].
- [77] E. W. Kolb and M. S. Turner, *The Early Universe*, vol. 69. 1990.
- [78] PLANCK Collaboration, N. Aghanim et al., *Planck 2018 results. I. Overview and the cosmological legacy of Planck*, *Astron. Astrophys.* **641** (2020) A1 [[1807.06205](#)].
- [79] BOSS Collaboration, S. Alam et al., *The clustering of galaxies in the completed SDSS-III Baryon Oscillation Spectroscopic Survey: cosmological analysis of the DR12 galaxy sample*, *Mon. Not. Roy. Astron. Soc.* **470** (2017) 2617 [[1607.03155](#)].
- [80] F. Beutler, C. Blake, M. Colless, D. H. Jones, L. Staveley-Smith, L. Campbell, Q. Parker, W. Saunders and F. Watson, *The 6dF Galaxy Survey: Baryon Acoustic Oscillations and the Local Hubble Constant*, *Mon. Not. Roy. Astron. Soc.* **416** (2011) 3017 [[1106.3366](#)].
- [81] A. J. Ross, L. Samushia, C. Howlett, W. J. Percival, A. Burden and M. Manera, *The clustering of the SDSS DR7 main Galaxy sample – I. A 4 per cent distance measure at $z = 0.15$* , *Mon. Not. Roy. Astron. Soc.* **449** (2015) 835 [[1409.3242](#)].
- [82] PLANCK Collaboration, N. Aghanim et al., *Planck 2018 results. V. CMB power spectra and likelihoods*, *Astron. Astrophys.* **641** (2020) A5 [[1907.12875](#)].
- [83] PLANCK Collaboration, N. Aghanim et al., *Planck 2018 results. VIII. Gravitational lensing*, *Astron. Astrophys.* **641** (2020) A8 [[1807.06210](#)].
- [84] S. Colombi, S. Dodelson and L. M. Widrow, *Large scale structure tests of warm dark matter*, *Astrophys. J.* **458** (1996) 1 [[astro-ph/9505029](#)].
- [85] K. Akita and M. Yamaguchi, *A precision calculation of relic neutrino decoupling*, *JCAP* **08** (2020) 012 [[2005.07047](#)].
- [86] J. J. Bennett, G. Buldgen, P. F. De Salas, M. Drewes, S. Gariazzo, S. Pastor and Y. Y. Y. Wong, *Towards a precision calculation of N_{eff} in the Standard Model II: Neutrino decoupling in the presence of flavour oscillations and finite-temperature QED*, *JCAP* **04** (2021) 073 [[2012.02726](#)].
- [87] D. Cadamuro, S. Hannestad, G. Raffelt and J. Redondo, *Cosmological bounds on sub-MeV mass axions*, *JCAP* **02** (2011) 003 [[1011.3694](#)].
- [88] D. Cadamuro and J. Redondo, *Cosmological bounds on pseudo Nambu-Goldstone bosons*, *JCAP* **02** (2012) 032 [[1110.2895](#)].
- [89] Y. Gong, A. Cooray, K. Mitchell-Wynne, X. Chen, M. Zemcov and J. Smidt, *Axion decay and anisotropy of near-IR extragalactic background light*, *Astrophys. J.* **825** (2016) 104 [[1511.01577](#)].
- [90] K. Kohri, T. Moroi and K. Nakayama, *Can decaying particle explain cosmic infrared background excess?*, *Phys. Lett. B* **772** (2017) 628 [[1706.04921](#)].
- [91] O. E. Kalashev, A. Kusenko and E. Vitagliano, *Cosmic infrared background excess from axionlike particles and implications for multimessenger observations of blazars*, *Phys. Rev. D* **99** (2019) 023002 [[1808.05613](#)].
- [92] A. Caputo, A. Vittino, N. Fornengo, M. Regis and M. Taoso, *Searching for axion-like particle*

- decay in the near-infrared background: an updated analysis, *JCAP* **05** (2021) 046 [[2012.09179](#)].
- [93] CAST Collaboration, M. Arik et al., *Search for Solar Axions by the CERN Axion Solar Telescope with ^3He Buffer Gas: Closing the Hot Dark Matter Gap*, *Phys. Rev. Lett.* **112** (2014) 091302 [[1307.1985](#)].
 - [94] J. Galán et al., *Exploring 0.1–10 eV axions with a new helioscope concept*, *JCAP* **12** (2015) 012 [[1508.03006](#)].
 - [95] I. G. Irastorza et al., *Gaseous time projection chambers for rare event detection: Results from the T-REX project. I. Double beta decay*, *JCAP* **01** (2016) 033 [[1512.07926](#)].
 - [96] J. Castel et al., *Background assessment for the TREX Dark Matter experiment*, *Eur. Phys. J. C* **79** (2019) 782 [[1812.04519](#)].
 - [97] J. Castel et al., *The TREX-DM experiment at the Canfranc Underground Laboratory*, *J. Phys. Conf. Ser.* **1468** (2020) 012063 [[1910.13957](#)].
 - [98] E. A. Paschos and K. Zioutas, *A Proposal for solar axion detection via Bragg scattering*, *Phys. Lett. B* **323** (1994) 367.
 - [99] SOLAX Collaboration, F. T. Avignone et al., *Solar axion experiments using coherent Primakoff conversion in single crystals*, *Nucl. Phys. B Proc. Suppl.* **72** (1999) 176.
 - [100] D. Li, R. J. Creswick, F. T. Avignone and Y. Wang, *Theoretical Estimate of the Sensitivity of the CUORE Detector to Solar Axions*, *JCAP* **10** (2015) 065 [[1507.00603](#)].
 - [101] E. Guarini, P. Carenza, J. Galan, M. Giannotti and A. Mirizzi, *Production of axionlike particles from photon conversions in large-scale solar magnetic fields*, *Phys. Rev. D* **102** (2020) 123024 [[2010.06601](#)].
 - [102] L. Di Luzio, F. Mescia, E. Nardi, P. Panci and R. Ziegler, *Astrophobic Axions*, *Phys. Rev. Lett.* **120** (2018) 261803 [[1712.04940](#)].
 - [103] A. Salvio, *A Simple Motivated Completion of the Standard Model below the Planck Scale: Axions and Right-Handed Neutrinos*, *Phys. Lett. B* **743** (2015) 428 [[1501.03781](#)].
 - [104] A. Salvio and S. Scollo, *Axion-Sterile-Neutrino Dark Matter*, [2104.01334](#).
 - [105] G. Gelmini, S. Palomares-Ruiz and S. Pascoli, *Low reheating temperature and the visible sterile neutrino*, *Phys. Rev. Lett.* **93** (2004) 081302 [[astro-ph/0403323](#)].
 - [106] G. Gelmini, E. Osoba, S. Palomares-Ruiz and S. Pascoli, *MeV sterile neutrinos in low reheating temperature cosmological scenarios*, *JCAP* **10** (2008) 029 [[0803.2735](#)].
 - [107] C. Benso, V. Brdar, M. Lindner and W. Rodejohann, *Prospects for Finding Sterile Neutrino Dark Matter at KATRIN*, *Phys. Rev. D* **100** (2019) 115035 [[1911.00328](#)].